

Tunnel ionization of H_2 in a low-frequency laser field: A wave-packet approach

T.-T. Nguyen-Dang, F. Châteauneuf, and S. Manoli
Département de Chimie, Université Laval, Québec, Canada G1K 7P4

O. Atabek and A. Keller
Laboratoire de Photophysique Moléculaire, CNRS, Bâtiment 213, Campus d'Orsay, 91405 Orsay Cedex, France
(Received 24 June 1996; revised manuscript received 21 May 1997)

The dynamics of multielectron dissociative ionization (MEDI) of H_2 in an intense IR laser pulse are investigated using a wave-packet propagation scheme. The electron tunneling processes corresponding to the successive ionizations of H_2 are expressed in terms of field-free Born-Oppenheimer (BO) potential energy surfaces (PES) by transforming the tunnel shape resonance picture into a Feshbach resonance problem. This transformation is achieved by defining a new, time-dependent electronic basis in which the bound electrons are still described by field-free BO electronic states while the ionized ones are described by Airy functions. In the adiabatic, quasistatic approximation, these functions describe free electrons under the influence of the instantaneous electric field of the laser and such an ionized electron can have a negative total energy. As a consequence, when dressed by the continuous ejected electron energy, the BO PES of an ionic channel can be brought into resonance with states of the parent species. This construction gives a picture in which wave packets are to be propagated on a continuum of coupled electronic manifolds. A reduction of the wave-packet propagation scheme to an effective five-channel problem has been obtained for the description of the first dissociative ionization process in H_2 by using Fano's formalism [U. Fano, *Phys. Rev.* **124**, 1866 (1961)] to analytically diagonalize the infinite, continuous interaction potential matrix and by using the properties of Fano's solutions. With this algorithm, the effect that continuous ionization of H_2 has on the dissociation dynamics of the H_2^+ ion has been investigated. In comparison with results that would be obtained if the first ionization of H_2 was impulsive, the wave-packet dynamics of the H_2^+ ion prepared continuously by tunnel ionization are markedly nonadiabatic. The continuous ionization appears to give rise to a population in the dissociative continuum that is localized at small internuclear distances throughout the action of the laser pulse, and is released only when the laser pulse is over, yielding a complex fragment kinetic energy spectrum. Comparison with available experimental data is made. [S1050-2947(97)04409-0]

PACS number(s): 42.50.Vk, 42.50.Hz, 33.80.Ps, 33.80.Gj

I. INTRODUCTION

The dynamics of multielectron dissociative ionization (MEDI) of laser-driven molecules have recently been of great interest in intense-field molecular physics [1–5]. One of the many issues yet to be elucidated in this context is the precise interplay between the multiple laser-induced ionization and dissociation pathways of the driven molecule. Experiments performed on N_2 [2] indicate that the successive ionizations occur at certain critical internuclear distances larger than the ground-state equilibrium bond length, suggesting a sequence of events in which vertical ionizations alternate with large-amplitude nuclear motions. More recent experiments on Cl_2 [4] and I_2 [5] suggest rather that the successive multiple ionization steps occur at a fixed, critical internuclear distance close to the neutral ground-state's equilibrium bond length. A tendency for the molecule under study to be stabilized with respect to dissociation as it undergoes this sequence of events in the course of its Coulomb explosion has been proposed to explain these observations. This hypothesis is further supported by pump-probe studies of MEDI on the same systems [6]. That multiple ionizations occur preferentially at a critical internuclear distance has also been rationalized in terms of an ionization enhancement effect reflecting rather a nonadiabatic electron localization process. This has been established by two recent independent

theoretical investigations of the dependence of the ionization rate of simple one-electron molecules on the nuclear geometry [7–10]. An experimental demonstration of the enhanced ionization effect has also been reported [11]. These works give indications that a tunnel mechanism for the ionization steps holds even in a high-frequency regime.

For the lightest molecular system that can undergo a MEDI process, the two-electron H_2 molecule, only two ionization steps are required for its complete explosion. Recent experimental works using an IR laser field suggest that the same type of sequential mechanism as that proposed for the heavier molecules governs the Coulomb explosion of H_2 [12] and D_2 [13]. This sequential mechanism is illustrated in Fig. 1. To interpret the experimentally observed monoenergetic proton kinetic energy spectra, it was proposed that these fragments originate from the Coulomb explosion occurring at a large internuclear distance (step 3 in Fig. 1). This distance is thought to be reached after nuclear motions of large amplitude of the laser-driven H_2^+ ion, (step 2 in Fig. 1). These motions would nevertheless carry insufficient momentum to be extended to the dissociative limit so that the formation of the same fragments by a laser-induced dissociation of the singly ionized species H_2^+ does not occur. As for the preparation of the H_2^+ ion, step 1 in Fig. 1, and the second ionization, step 3 in this figure, a tunnel mechanism was suggested because multiphoton ionizations would require

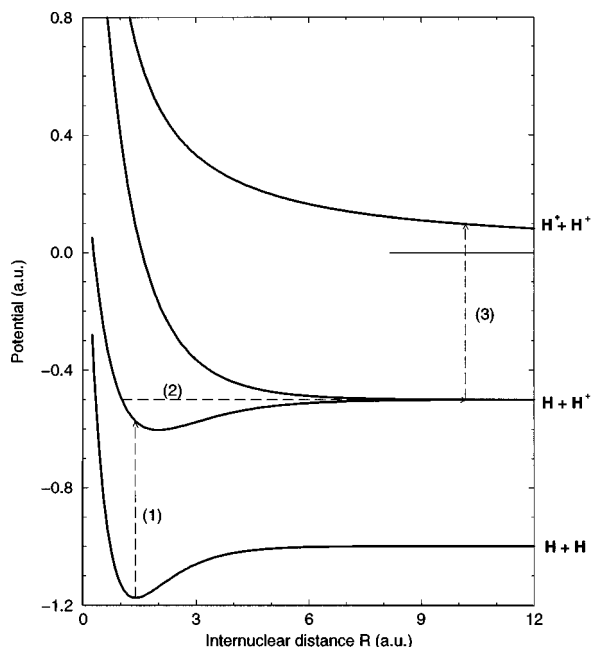


FIG. 1. Sequential mechanism for the complete Coulomb explosion of H₂. Arrow (1) corresponds to the tunnel ionization of the neutral molecule, arrow (2) corresponds to the laser-induced dissociation of the molecular ion H₂⁺, and arrow (3) corresponds to the second tunnel ionization that brings the system on the repulsive curve of the doubly ionized species.

over a hundred photons of the IR incident laser field in each case. From an adaptation of a popular theory for tunnel ionization, due to Ammosov, Delone, and Krainov (ADK theory) [14], to a molecular system, it is also inferred that the second ionization step most probably occurs at a large internuclear distance rather than in the neighborhood of the equilibrium position. This is consistent with the recent theoretical predictions of enhanced tunnel ionization at large internuclear distances [7–10].

It has been suggested [12] that the proposed large-amplitude nuclear motions of the singly ionized species, i.e., step 2 in Fig. 1, result from classical chaotic dissociation dynamics [15,16]. To obtain the precise details of this transient nuclear dynamics, a wave-packet simulation of step 2 alone has been performed in a preliminary investigation of the Coulomb explosion mechanism. While the salient features of this study will be described in some detail in Sec. V, a more complete account of this work will be reported elsewhere [17]. In this study, an initial wave packet arbitrarily prepared by vertical promotion of the $v=0$ vibrational ground state of the neutral molecule onto the $2^2\Sigma_g^+$ ground-state manifold of the H₂⁺ ion was propagated on the coupled charge exchange states, $2^2\Sigma_g^+$ and $2^2\Sigma_u^+$, of the ion. Vibrational excitation above and beyond that contained in the initial nonstationary wave packet was found [17]. Since this homonuclear system possesses no permanent dipole moment, the observed vibrational excitation is an effective consequence of nonresonant electronic excitation of the ion in the IR field. The vibrational excitation is accompanied by a quenching of the dissociation probability, the extent of which depends critically on the initial conditions. This last observation will be illustrated in Sec. V. It demonstrates the importance of a more complete description, which would prop-

erly include the first ionization process as a continuous source of initial wave packets for step 2.

In attempting to include this continuous first tunnel ionization step, an interesting theoretical and conceptual problem arises: the tunnel mechanism refers to the electronic penetration of the barrier, which is created by superimposing a linear potential denoting the interaction between the electron and the laser field on the Coulomb potential [1]. Because of this deformation of the Coulomb potential, a set of shape resonances replaces the field-free Born-Oppenheimer (BO) states and their nuclear-configuration-dependent complex energies define new potential energy surfaces (PES). In other words, the concept of tunnel ionization is obscured within an interpretation such as depicted in Fig. 1, which employs the field-free BO PES's. It is clear that to obtain a representation of the electron tunneling processes in terms of field-free BO PES's, a projection of the aforementioned new time-dependent adiabatic electronic states onto the field-free states is needed. This is difficult because, in principle, each of the new adiabatic electronic states associated with the tunnel shape-resonance problem projects onto an infinite number of field-free states. Moreover, *a priori*, these shape resonance states are as yet unknown.

Given the difficulties outlined above, the projection of the tunnel dynamical picture onto the field-free BO picture is clearly a nontrivial problem. The present paper proposes a scheme to treat this problem. Recognizing that electrons ionized during the action of the laser pulse are not free, but continue to feel the driving force of the field, a time-dependent electronic basis is constructed. In this basis, the bound states of both the neutral and ionic species are still described by field-free BO electronic states while the ionized electrons are described by scattering wave functions that asymptotically behave as Airy functions, i.e., as eigenfunctions of an electron driven linearly by a quasistatic field. An ionized electron can thus have negative total energy as opposed to the field-free situation where its energy is purely of a kinetic nature and is always positive. As a consequence, when dressed by the continuous ejected electron energy, the BO PES's of the ionic channels can be brought into resonance with the ground state of the parent species, yielding a Feshbach resonance picture of the tunnel ionization process. In this way, the wave-packet dynamics of tunnel ionization can be described using the field-free BO PES's. The construction of the new electronic basis introduces an asymmetry in the treatment of bound and free electrons. A similar asymmetry was found in previous calculations of the tunnel ionization rates of atoms using a scattering matrix formalism [18–20]: while the initial bound electron was described by field-free eigenstates, its final state was described by Volkov states or by Coulomb-Volkov states, which denote the scattering of a laser-driven electron by a Coulomb center [21]. In the present treatment, Airy functions correspond to Volkov states in a quasistatic picture, and Coulomb-Airy functions, i.e., Coulomb scattering functions with an Airy-function asymptotic behavior, correspond to Coulomb-Volkov states. Note that in any wave-packet propagation technique, such as the celebrated third-order split-operator algorithm [22] applied to a time-dependent Hamiltonian, a quasistatic picture is implicitly invoked. Thus, in the present molecular wave-packet study of the dissociative ionization of H₂, this implicit

quasistatic picture imposes the use of these approximate, time-dependent, adiabatic states as replacements of the exact Volkov or Coulomb-Volkov states. They ensure a consistent treatment of the time evolution of the system, electrons and nuclei taken altogether.

This formulation of the wave-packet dynamics of tunnel ionization, which yields a picture in which wave packets are propagated on a continuum of coupled electronic manifolds, gives rise to a new technical challenge. In a minimal basis needed for the proper description of the step 1 and step 2 in Fig. 1, where a single state, viz., the ground state, of the neutral molecule, is kept along with the two charge exchange states of the singly ionized species, the formalism gives two continua of ionized channels, obtained by dressing the two field-free PES's of the H_2^+ ion with the single free electron's energy. In their present forms, wave-packet propagation techniques are suitable only for problems involving a finite number of channels [23–25,22]. An adaptation of these techniques to the situations involving a continuum of channels is thus required. In the present work, the third-order split-operator algorithm [22] is adapted, and the diagonalization of the potential matrix describing the bound-free channel couplings is achieved analytically by using Fano's formalism [26]. Insofar as the bound-free couplings are not too strongly energy dependent, this analytical solution turns out to be quite useful as it reduces the problem to an effective five-channel problem. This reduction denotes the well-known localization of bound-free population exchanges to “on-the-energy-shell” transitions in the neighborhood of the associated Feshbach resonances. It is interesting to note that the Fano formalism has previously been used only in the context of a time-independent stationary state. The present paper represents an attempt to adapt it for a time-dependent wave-packet description. The resulting algorithm is used to assess the effects that continuous tunnel ionization can have on the laser-induced wave-packet dynamics in H_2^+ . One effect that this continuous ionization appears to have is a slight enhancement of the stabilization of the molecular ion toward its dissociation, as compared to the situation already present in the dynamics of step 2 alone. This effect denotes a strong coupling between ionization and dissociation, which are induced by the laser field in this light molecular system.

II. TUNNEL IONIZATION AS A FESHBACH RESONANCE PROBLEM

To fully describe the events occurring during the Coulomb explosion of H_2 , the time-dependent Schrödinger equation

$$i\hbar \partial_t |\Psi, t\rangle = \hat{H}_{\text{tot}}(t) |\Psi, t\rangle \quad (1)$$

must be solved. Here

$$\hat{H}_{\text{tot}}(t) \equiv \hat{T}_N + \hat{H}_{\text{el}}(t), \quad (2)$$

$$\hat{H}_{\text{el}}(t) = \hat{T}_e + V_{\text{Coul}}(\vec{r}_1, \vec{r}_2 | \vec{R}) - e\vec{\mathcal{E}}(t) \cdot (\vec{r}_1 + \vec{r}_2), \quad (3)$$

where $\vec{\mathcal{E}}(t)$ is the laser field, \hat{T}_N, \hat{T}_e denote the kinetic energy operators for the nuclear and electronic motions, respectively, and V_{Coul} is the sum of all Coulomb interactions between the charges

$$V_{\text{Coul}}(\vec{r}_1, \vec{r}_2 | \vec{R}) \equiv - \sum_{i=1}^2 \left(\frac{e^2}{|\vec{r}_i - \vec{R}/2|} + \frac{e^2}{|\vec{r}_i + \vec{R}/2|} \right) + \frac{e^2}{|\vec{r}_{12}|} + \frac{e^2}{|\vec{R}|}. \quad (4)$$

Note that the long-wavelength approximation (LWA) was used within the so-called electric-field (EF) gauge (or length gauge) [27] where radiative interactions are given by the last term of Eq. (3). In addition, Jacobi coordinates for the four-body problem were used and the center-of-mass motion had been implicitly factored out. Thus, the time-dependent part of the Hamiltonian \hat{H}_{tot} denotes the interaction between the laser field and the relative electronic motions only since the relative nuclear motions do not interact with the laser field due to the inversion symmetry of this homonuclear system.

For a slowly varying $\vec{\mathcal{E}}(t)$, such as a low-frequency field, an adiabatic *electronic* basis [28] incorporating the interaction term of Eq. (3) may be used to replace the traditional field-free BO basis. The addition of the radiative interaction term to the attractive Coulomb field gives rise to a barrier, and the electronic motion across this barrier corresponds to a tunnel ionization process [1]. The challenge is to obtain a representation of the same dynamical processes in terms of field-free BO PES's. This amounts to translating the shape-resonance problem associated with the tunnel picture into a Feshbach-resonance problem involving interactions between field-free BO states. To achieve this, it is useful to construct a new basis in the following manner: the bound electronic states of both the neutral and singly ionized species will continue to be represented by the associated field-free wave functions, denoted by $\psi_I^{\text{H}_2}$ and $\psi_J^{\text{H}_2^+}$, while the ionized electron(s) will be represented by a wave function \mathcal{A}_E denoting a free particle scattered by a Coulomb potential in a quasistatic electric field. Thus, in the simplest approximation, ignoring the Coulomb field, these would simply be the Airy functions defined by

$$\left\{ \frac{\hat{p}_e^2}{2m_e} - e\vec{\mathcal{E}} \cdot \vec{r} \right\} \text{Ai}(\vec{r}, t | E) = E \text{Ai}(\vec{r}, t | E). \quad (5)$$

The introduction of these wave functions amounts to recognizing that after its ejection, the ionized electron still feels the influence of the laser field. It can be easily recognized that the wave functions $\text{Ai}(\vec{r}, t | E)$ defined in Eq. (5) correspond to the Volkov states in the quasistatic limit. Including the nuclear Coulomb attraction in the single-electron Hamiltonian appearing on the left-hand side of Eq. (5) defines what will be referred to as Airy-Coulomb wave functions. Formally, these are states describing the scattering of an electron by a multicenter Coulomb potential in the presence of a static electric field \mathcal{E} . In the quasistatic limit, these correspond to the Volkov-Coulomb states introduced recently by Reiss and Krainov [21]. Henceforth, the notation \mathcal{A}_E will be used to denote these scattering states, keeping in mind their

asymptotic behavior described by Eq. (5). Having defined these wave functions for the ionized electrons, a nonorthogonal electronic basis is obtained:

$$\mathcal{B} \equiv \{ \psi_I^{\text{H}_2}(1,2) \} \cup \{ | \psi_I^{\text{H}_2^+}(1) \bar{\mathcal{A}}_E(2) | \} \cup \{ | \mathcal{A}_E(1) \bar{\mathcal{A}}_E(2) | \}, \quad (6)$$

where 1 and 2 are abbreviations for the coordinate and spin of the two electrons, and standard quantum-chemical notations are used: $|\phi \bar{\eta}|$ denotes the antisymmetrized product $[\phi(1)\bar{\eta}(2) - \bar{\eta}(1)\phi(2)]/\sqrt{2}$ and the bar above η indicates an electron spin component $m_s = -1/2$. Expanding the total time-dependent wave function $\Psi_{\text{tot}}(1,2,R,t)$ in this basis

$$\Psi_{\text{tot}} = \sum_I \chi_I^{\text{H}_2}(R,t) \psi_I^{\text{H}_2}(1,2) + \sum_J \int dE \chi_{JE}^{\text{H}_2^+}(R,t) | \psi_I^{\text{H}_2^+}(1) \bar{\mathcal{A}}_E(2) | + \int dE \int dE' \chi_{EE'}^{\text{H}_2^{++}}(R,t) | \mathcal{A}_E(1) \bar{\mathcal{A}}_E(2) | \quad (7)$$

the following set of coupled equations for the nuclear amplitudes $\chi_I^{\text{H}_2}$, $\chi_{JE}^{\text{H}_2^+}$, and $\chi_{EE'}^{\text{H}_2^{++}}$ is obtained from Eq. (1)

$$\begin{aligned} i\hbar \dot{\chi}_I^{\text{H}_2} = & (\hat{T}_N + \varepsilon_I) \chi_I^{\text{H}_2} + \sum_{I' \neq I} \langle \psi_I^{\text{H}_2} | -e\vec{E}(t) \cdot (\vec{r}_1 + \vec{r}_2) | \psi_{I'}^{\text{H}_2} \rangle \chi_{I'}^{\text{H}_2} + \sum_J \int dE \{ (\hat{T}_N \chi_{JE}^{\text{H}_2^+} - i\hbar \dot{\chi}_{JE}^{\text{H}_2^+}) \langle \psi_I^{\text{H}_2} | \psi_J^{\text{H}_2^+} \bar{\mathcal{A}}_E \rangle \\ & + \langle \psi_I^{\text{H}_2} | \hat{H}_{\text{el}}(t) | \psi_J^{\text{H}_2^+} \bar{\mathcal{A}}_E \rangle \chi_{JE}^{\text{H}_2^+} \} + \int dE \int dE' \{ (\hat{T}_N \chi_{EE'}^{\text{H}_2^{++}} - i\hbar \dot{\chi}_{EE'}^{\text{H}_2^{++}}) \langle \psi_I^{\text{H}_2} | \mathcal{A}_E \bar{\mathcal{A}}_{E'} \rangle + \langle \psi_I^{\text{H}_2} | \hat{H}_{\text{el}}(t) | \mathcal{A}_E \bar{\mathcal{A}}_{E'} \rangle \chi_{EE'}^{\text{H}_2^{++}} \}, \end{aligned} \quad (8a)$$

$$\begin{aligned} i\hbar \dot{\chi}_{JE}^{\text{H}_2^+} = & (\hat{T}_N + \varepsilon_J + E) \chi_{JE}^{\text{H}_2^+} + \sum_{J' \neq J} \langle \psi_J^{\text{H}_2^+} | -eE(t) \cdot \vec{r}_1 | \psi_{J'}^{\text{H}_2^+} \rangle \chi_{J'E}^{\text{H}_2^+} + \sum_{J'} \int dE' \langle JE | V_{ee} | J'E' \rangle \chi_{J'E'}^{\text{H}_2^+} + \sum_I \{ (\hat{T}_N \chi_I^{\text{H}_2} - i\hbar \dot{\chi}_I^{\text{H}_2}) \\ & \times \langle \psi_J^{\text{H}_2^+} \bar{\mathcal{A}}_E | \psi_I^{\text{H}_2} \rangle + \langle \psi_J^{\text{H}_2^+} \bar{\mathcal{A}}_E | \hat{H}_{\text{el}}(t) | \psi_I^{\text{H}_2} \rangle \chi_I^{\text{H}_2} \} + \int dE \int dE' \{ (\hat{T}_N \chi_{EE'}^{\text{H}_2^{++}} - i\hbar \dot{\chi}_{EE'}^{\text{H}_2^{++}}) \langle \psi_J^{\text{H}_2^+} \bar{\mathcal{A}}_E | \mathcal{A}_E \bar{\mathcal{A}}_{E'} \rangle \\ & + \langle \psi_J^{\text{H}_2^+} \bar{\mathcal{A}}_E | \hat{H}_{\text{el}}(t) | \mathcal{A}_E \bar{\mathcal{A}}_{E'} \rangle \chi_{EE'}^{\text{H}_2^{++}} \}, \end{aligned} \quad (8b)$$

$$\begin{aligned} i\hbar \dot{\chi}_{EE'}^{\text{H}_2^{++}} = & (\hat{T}_N + E + E' + V_{nn}) \chi_{EE'}^{\text{H}_2^{++}} + \int dE'' \int dE''' \langle EE' | V_{ee} | E''E''' \rangle \chi_{E''E'''}^{\text{H}_2^{++}} + \sum_I \{ (\hat{T}_N \chi_I^{\text{H}_2} - i\hbar \dot{\chi}_I^{\text{H}_2}) \langle \mathcal{A}_E \bar{\mathcal{A}}_{E'} | \psi_I^{\text{H}_2} \rangle \\ & + \langle \mathcal{A}_E \bar{\mathcal{A}}_{E'} | \hat{H}_{\text{el}}(t) | \psi_I^{\text{H}_2} \rangle \chi_I^{\text{H}_2} \} + \sum_J \int dE'' \{ (\hat{T}_N \chi_{JE''}^{\text{H}_2^+} - i\hbar \dot{\chi}_{JE''}^{\text{H}_2^+}) \langle \mathcal{A}_E \bar{\mathcal{A}}_{E'} | \psi_J^{\text{H}_2^+} \bar{\mathcal{A}}_{E''} \rangle + \langle \mathcal{A}_E \bar{\mathcal{A}}_{E'} | \hat{H}_{\text{el}}(t) | \psi_J^{\text{H}_2^+} \bar{\mathcal{A}}_{E''} \rangle \chi_{JE''}^{\text{H}_2^+} \}. \end{aligned} \quad (8c)$$

In these equations, $\langle JE | V_{ee} | J'E' \rangle$ or $\langle EE' | V_{ee} | E''E''' \rangle$ represents a matrix element of the two-electron Coulomb repulsion operator $V_{ee}(1,2) \equiv e^2/r_{12}$, between a pair of singly ionized states $|\psi_J^{\text{H}_2^+} \bar{\mathcal{A}}_{E'} \rangle$ or a pair of doubly ionized states $|\mathcal{A}_E \bar{\mathcal{A}}_{E'} \rangle$, respectively. In the spirit of the adiabatic approximation, which is justified by the low-frequency condition considered presently, the nonadiabatic coupling terms arising from the time dependence of the continuum single-electron wave functions, \mathcal{A}_E , have been neglected [29]. Also, nonradiative couplings associated with the possible breakdown of the Born-Oppenheimer approximation are neglected to focus on the radiative interactions.

The first observation that can be made at this point is the existence of coupling terms of the form

$$(\hat{T}_N \chi_{JE}^{\text{H}_2^+} - i\hbar \dot{\chi}_{JE}^{\text{H}_2^+}) \langle \psi_I^{\text{H}_2} | \psi_J^{\text{H}_2^+} \bar{\mathcal{A}}_E \rangle,$$

$$(\hat{T}_N \chi_{JE''}^{\text{H}_2^+} - i\hbar \dot{\chi}_{JE''}^{\text{H}_2^+}) \langle \mathcal{A}_E \bar{\mathcal{A}}_{E'} | \psi_J^{\text{H}_2^+} \bar{\mathcal{A}}_{E''} \rangle, \quad \text{etc.}$$

These arise from the nonorthogonal nature of the basis \mathcal{B} [30], and are irrelevant. To see this, it is convenient to formally rewrite the set of coupled equations (8a)–(8c) in matrix form. Defining \underline{X} to be the infinite vector containing the amplitudes $\chi_I^{\text{H}_2}$, $\chi_{JE}^{\text{H}_2^+}$, etc., $\underline{\mathcal{S}}$ the matrix of overlap integrals between the vectors of the basis \mathcal{B} and $\underline{H}_{\text{el}}$, the matrix representation of $\hat{H}_{\text{el}}(t)$ in this basis, Eqs. (8a)–(8c) can be written as

$$i\hbar \underline{\mathcal{S}} \partial_t \underline{X} = \underline{\mathcal{S}} (\hat{T}_N \underline{X}) + \underline{H}_{\text{el}} \underline{X}. \quad (9)$$

Multiplying this by $\underline{\mathcal{S}}^{-1}$ gives

$$i\hbar \partial_t \underline{X} = (\hat{T}_N \underline{\mathcal{I}} + \underline{\mathcal{S}}^{-1} \underline{H}_{\text{el}}) \underline{X}, \quad (10)$$

whereby the coupling terms involving the overlap integrals $\langle \mathcal{A}_E \bar{\mathcal{A}}_{E'} | \psi_J^{\text{H}_2^+} \bar{\mathcal{A}}_{E''} \rangle$ or $\langle \psi_I^{\text{H}_2} | \psi_J^{\text{H}_2^+} \bar{\mathcal{A}}_E \rangle$, etc., are completely removed.

The second observation to be made about Eqs. (8a), (8b), and (8c) is the dressing of the PES's, ε_J , of H_2^+ by the

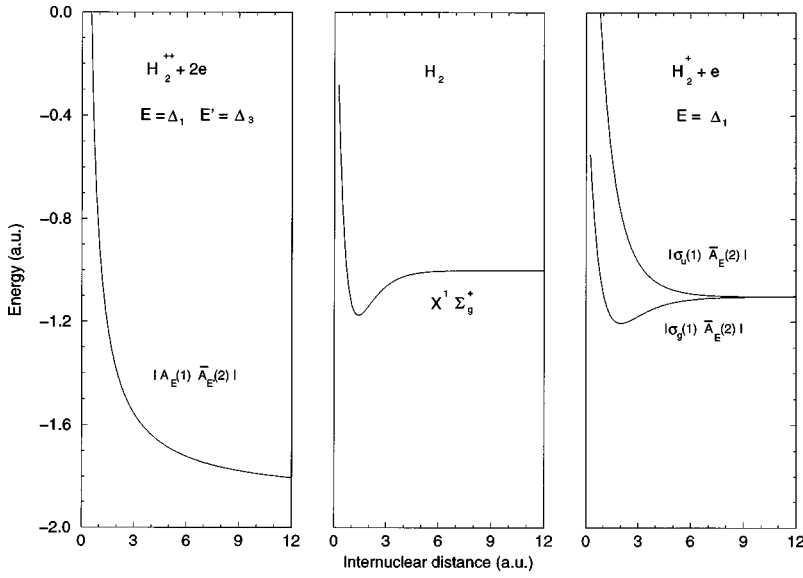


FIG. 2. Dressing of the PES's, ϵ_j , $j=1,2$, of H_2^+ by the energy E of the first ionized electron, and of the PES $V_{nn}(R)$ of H_2^{2+} by the energies E, E' of the two ionized electrons. $E = \Delta_1$, $E' = \Delta_3$, where $-\Delta_1$ and $-\Delta_3$ are the first and second ionization potentials of H_2 .

energy E of the first electron to be ionized, while the PES's of H_2^{2+} , the pure nuclear Coulomb potential $V_{nn}(R)$, is dressed by the energies E, E' of the two ionized electrons. This dressing is illustrated in Fig. 2 for the particular values $E = \Delta_1$, $E' = \Delta_3$, where $-\Delta_1$ and $-\Delta_3$ are the first and second ionization potentials of H_2 . As seen in this figure, the dressing causes the PES's of the ionic channels to be repositioned in such a manner as to offer resonant bound-free interactions. This is the Feshbach representation of the tunnel ionization process alluded to above. For a low-frequency field, such as IR laser source, the resonant transitions caused by these interactions will be favored over the highly nonresonant bound-bound transitions.

Within the description using the nonorthogonal basis \mathcal{B} of Eq. (6), the bound-free couplings are contained in the matrix $\underline{S}^{-1} \underline{H}_{el}$. They are governed by the matrix elements

$$\begin{aligned} \langle \psi_I^{H_2} | \hat{H}_{el}(t) | \psi_J^{H_2^+} \bar{\mathcal{A}}_E \rangle &= \epsilon_I^{H_2} \langle \psi_I^{H_2} | \psi_J^{H_2^+} \bar{\mathcal{A}}_E \rangle \\ &\quad - e \tilde{\mathcal{E}}(t) \cdot \langle \psi_I^{H_2} | (\vec{r}_1 + \vec{r}_2) | \psi_J^{H_2^+} \bar{\mathcal{A}}_E \rangle \end{aligned} \quad (11)$$

for the first ionization step and

$$\begin{aligned} \langle \psi_J^{H_2^+} \bar{\mathcal{A}}_E | \hat{H}_{el}(t) | \mathcal{A}_{E'} \bar{\mathcal{A}}_{E''} \rangle & \\ = \{ (\epsilon_J^{H_2^+} + E) \langle \psi_J^{H_2^+} | \mathcal{A}_{E'} \rangle - e \tilde{\mathcal{E}}(t) \cdot \langle \psi_J^{H_2^+} | \vec{r}_1 | \mathcal{A}_{E'} \rangle \} & \\ \times \delta(E - E'') & \end{aligned} \quad (12)$$

for the second ionization step.

Thus with $I=0$, corresponding to the ground state of H_2 , $\psi_0^{H_2} = |1\sigma_g^{H_2} 1\sigma_g^{H_2}\rangle$ and $J=0$ and 1 corresponding to the ground state, $1\sigma_g^{H_2^+}$, and first excited state, $1\sigma_u^{H_2^+}$, respectively, of H_2^+ , the Condon-Slater rules [31] give

$$\begin{aligned} \langle \psi_0^{H_2} | \hat{H}_{el}(t) | \psi_0^{H_2^+} \bar{\mathcal{A}}_E \rangle & \\ = \epsilon_0^{H_2} \langle 1\sigma_g^{H_2} | \mathcal{A}_E \rangle \langle 1\sigma_g^{H_2} | 1\sigma_g^{H_2^+} \rangle - e \tilde{\mathcal{E}}(t) \cdot (\langle 1\sigma_g^{H_2} | \vec{r}_1 | \mathcal{A}_E \rangle & \\ \times \langle 1\sigma_g^{H_2} | 1\sigma_g^{H_2^+} \rangle + \langle 1\sigma_g^{H_2} | \mathcal{A}_E \rangle \langle 1\sigma_g^{H_2} | \vec{r}_1 | 1\sigma_g^{H_2^+} \rangle), & \end{aligned} \quad (13a)$$

$$\begin{aligned} \langle \psi_0^{H_2} | \hat{H}_{el}(t) | \psi_1^{H_2^+} \bar{\mathcal{A}}_E \rangle & \\ = \epsilon_0^{H_2} \langle 1\sigma_g^{H_2} | \mathcal{A}_E \rangle \langle 1\sigma_g^{H_2} | 1\sigma_u^{H_2^+} \rangle - e \tilde{\mathcal{E}}(t) \cdot (\langle 1\sigma_g^{H_2} | \vec{r}_1 | \mathcal{A}_E \rangle & \\ \times \langle 1\sigma_g^{H_2} | 1\sigma_u^{H_2^+} \rangle + \langle 1\sigma_g^{H_2} | \mathcal{A}_E \rangle \langle 1\sigma_g^{H_2} | \vec{r}_1 | 1\sigma_u^{H_2^+} \rangle), & \end{aligned} \quad (13b)$$

$$\begin{aligned} \langle \psi_0^{H_2^+} \bar{\mathcal{A}}_E | \hat{H}_{el}(t) | \mathcal{A}_{E'} \bar{\mathcal{A}}_{E''} \rangle & \\ = \{ (\epsilon_0^{H_2^+} + E) \langle 1\sigma_g^{H_2^+} | \mathcal{A}_{E'} \rangle - e \tilde{\mathcal{E}}(t) \cdot \langle 1\sigma_g^{H_2^+} | \vec{r}_1 | \mathcal{A}_{E'} \rangle \} & \\ \times \delta(E - E'') & \end{aligned} \quad (13c)$$

It is clear that these matrix elements are governed by the degree of overlap between the Coulomb-Airy function \mathcal{A}_E and the molecular orbital from which the electron is ejected. For $R = R_{eq}$, the equilibrium geometry of H_2 in its ground state and within the approximation $\mathcal{A}_E \approx \text{Ai}(E)$, Fig. 3 shows the disposition of the relevant basis functions at $E = \Delta_1$, $E' = \Delta_3$, i.e., at electron energies ensuring a resonance condition for the first and second ionization steps of H_2 . It is seen that the overlap between the Airy function $\text{Ai}(E = \Delta_1)$ and the $1\sigma_g$ orbital of H_2 , while small [$O(10^{-5}$ a.u.)], is much more pronounced than that between $\text{Ai}(E = \Delta_3)$ and the $1\sigma_g$ orbital of H_2^+ [$O(10^{-24}$ a.u.)]. This implies that the first ionization step, operative at small R , can be considered separately from the second ionization step, which is operative only at some relatively large value of R . The same consideration also gives a justification for the neglect of the two-electron integrals $\langle JE | V_{ee} | J'E' \rangle$ when $J, J' = 0$ and 1. In the following, attention will be given exclusively to the first ionization step in the Coulomb explosion of H_2 and the minimal basis:

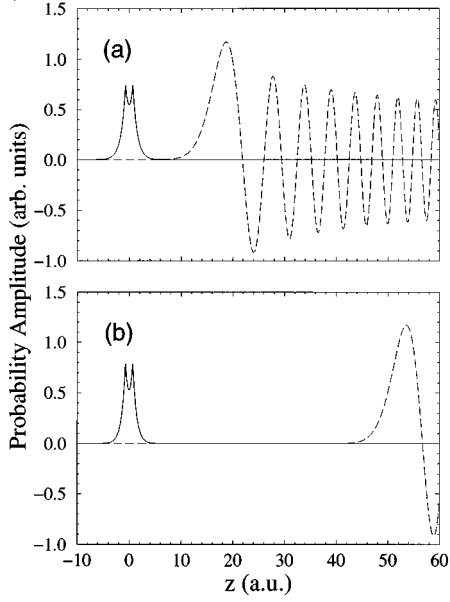


FIG. 3. Disposition of the Airy function $\text{Ai}(E)$ (dashed line) and the molecular orbitals $\sigma_g^{\text{H}_2}$ and $\sigma_g^{\text{H}_2^+}$ (solid line) involved in the first (a) and second (b) ionization steps of H₂, for which $E = \Delta_1$, $E = \Delta_3$, respectively. Note that the wave functions themselves are shown here, not their square moduli. The overlap matrix integral is evaluated to be 2.63×10^{-5} a.u. in (a) and 8.15×10^{-25} a.u. in (b).

$$\mathcal{B}' \equiv \{ \psi_0^{\text{H}_2}(1,2), |1\sigma_g^{\text{H}_2^+}(1)\bar{\mathcal{A}}_E(2)\rangle, |1\sigma_u^{\text{H}_2^+}(1)\bar{\mathcal{A}}_E(2)\rangle \} \quad (14)$$

will be used. As indicated, a single electronic state, the ground state of the neutral species, H₂, is kept in this basis, while the two charge-resonant states, $1\sigma_g^{\text{H}_2^+}$ and $1\sigma_u^{\text{H}_2^+}$, of H₂⁺ define the ionization continua, i.e., the final states of the first ionization process. These states interact with each other only via the transition dipole moment $\langle 1\sigma_g^{\text{H}_2^+} | \vec{r} | 1\sigma_u^{\text{H}_2^+} \rangle$, and interactions that are generated within the ionized continua by the electron repulsion potential are completely neglected by virtue of the above observation.

III. TIME EVOLUTION AND FANO REPRESENTATION

A. Split-operator formula

The solution of Eq. (9) or Eq. (10) can be obtained numerically by using any of the existing wave-packet propagation techniques such as the third-order split operator formula [22]. In the present context, the split operator formula gives

$$\begin{aligned} \underline{X}(t_0 + \delta t) = & \exp\left\{-\frac{i}{\hbar} \hat{T}_{N\bar{I}} \frac{\delta t}{2}\right\} \exp\left\{-\frac{i}{\hbar} \underline{S}^{-1} \underline{H}_{\text{el}} \delta t\right\} \\ & \times \exp\left\{-\frac{i}{\hbar} \hat{T}_{N\bar{I}} \frac{\delta t}{2}\right\} \underline{X}(t_0) + O(\delta t^3) \end{aligned} \quad (15)$$

as a short-time approximation to the solution of Eq. (10) evolving from an initial condition described by $\underline{X}(t_0)$. Current applications of this third-order split operator formula are restricted to problems involving a finite number of channels [8,32,33]. An extension to an infinite matrix case is found in the Floquet treatments of laser-driven multichannel molecu-

lar systems [34]. However, formally, the potential matrix involved in such problems is of infinite dimension but discrete whereas, here, $\underline{S}^{-1} \underline{H}_{\text{el}}$ is formally a matrix of infinite dimension, which is continuous, denoting two continua of R -parametrized electronic states interacting with a bound state. Its diagonalization requires a special analytical treatment. Let $\underline{\Omega}$ be the matrix that achieves this diagonalization, i.e.,

$$\underline{\Omega}^{-1} \underline{S}^{-1} \underline{H}_{\text{el}} \underline{\Omega} \equiv \underline{E} \quad (16)$$

so that Eq. (15) can be rewritten as

$$\begin{aligned} \underline{X}(t_0 + \delta t) = & \exp\left\{-\frac{i}{\hbar} \hat{T}_{N\bar{I}} \frac{\delta t}{2}\right\} \underline{\Omega} \exp\left\{-\frac{i}{\hbar} \underline{E} \delta t\right\} \underline{\Omega}^{-1} \\ & \times \exp\left\{-\frac{i}{\hbar} \hat{T}_{N\bar{I}} \frac{\delta t}{2}\right\} \underline{X}(t_0) + O(\delta t^3). \end{aligned} \quad (17)$$

In the form given by Eq. (16), the construction of $\underline{\Omega}$ is difficult, as the inversion of \underline{S} is rather cumbersome, due to the infinite, continuous character of the basis \mathcal{B} . To avoid this inversion, it is preferable to recast Eq. (16) into the canonical form of eigenvalue equation associated with a nonorthogonal basis

$$(\underline{H}_{\text{el}} - E_i \underline{S}) \underline{\Omega}_i = 0, \quad (18)$$

where $\underline{\Omega}_i$ is the i th column, associated with eigenvalue E_i , of the matrix $\underline{\Omega}$. To solve Eq. (18), the general approach developed by Fano [26] for eigenvalue problems involving continua can be exploited. Fano's formulation also allows for the successive action of the infinite continuous matrices $\underline{\Omega}^\dagger$ and $\underline{\Omega}$ in Eq. (17) to be evaluated analytically. However, it is to be noted that Fano's original formulation was expressed in terms of an orthogonal basis. Thus, an extension of this formalism to the present context is needed to account for the nonorthogonal character of the basis \mathcal{B}' .

B. Diagonalization of the coupling potential matrix: Fano representation

To simplify the notations, let $\epsilon_0(R)$, $\epsilon_1(R)$, and $\epsilon_2(R)$ be the Born-Oppenheimer energy of the electronic states in the minimal basis of Eq. (14), $V_{E'}$ the interaction between the ground channel ϵ_0 and the continuum $\epsilon_1 + E'$, $W_{E'}$ that between ϵ_0 and the continuum $\epsilon_2 + E'$, and V_{12} the radiative interaction between the two charge resonance states of H₂⁺. To manipulate symbolically the matrices in Eq. (15), a convention is needed for the ordering of the elements in the basis \mathcal{B}' . The following convention will henceforth be used systematically. The bound state $\psi_0^{\text{H}_2} = |1\sigma_g^{\text{H}_2} 1\sigma_g^{\text{H}_2}\rangle$ will always be the first element of the basis, followed successively by the infinite blocks $|1\sigma_g^{\text{H}_2^+} \bar{\mathcal{A}}_{E'}\rangle$ and $|1\sigma_u^{\text{H}_2^+} \bar{\mathcal{A}}_{E'}\rangle$, the ionized electron's energy E' ranging continuously from $-\infty$ to $+\infty$, in principle. Although this energy, which labels the continuum basis states, varies continuously, all infinite matrices to be found in the following are written in a discrete infinite form, for ease of representation; no discretizations of the continua are implied by this convention. Let the elements in a column of $\underline{\Omega}$ (labeled by E) be denoted $a(E)$,

$\beta_{E'}(E)$, $\gamma_{E'}(E)$. Then, according to Eq. (18), they are solutions of the following system of equations:

$$\begin{aligned} \epsilon_0 a(E) + \int dE' [(V_{E'}^* - ES_{1E'}^*) \beta_{E'}(E) \\ + (W_{E'}^* - ES_{1E'}^*) \gamma_{E'}(E)] = Ea(E), \end{aligned} \quad (19a)$$

$$\begin{aligned} (V_{E'} - ES_{1E'}) a(E) + (\epsilon_1 + E') \beta_{E'}(E) + V_{12} \gamma_{E'}(E) \\ = E \beta_{E'}(E), \end{aligned} \quad (19b)$$

$$\begin{aligned} (W_{E'} - ES_{1E'}) a(E) + V_{12}^* \beta_{E'}(E) + (\epsilon_2 + E') \gamma_{E'}(E) \\ = E \beta_{E'}(E), \end{aligned} \quad (19c)$$

satisfying the orthonormalization condition

$$\begin{aligned} a^*(E) a(E'') + \int dE' [\beta_{E'}^*(E) \beta_{E'}(E'') + \gamma_{E'}^*(E) \gamma_{E'}(E'')] \\ + a^*(E) \beta_{E'}(E'') S_{1E'} + a(E'') \beta_{E'}^*(E) S_{1E'}^* \\ + a^*(E) \gamma_{E'}(E'') S_{2E'} + a(E'') \gamma_{E'}^*(E) S_{2E'}^* \\ = \delta(E'' - E). \end{aligned} \quad (20)$$

To be more precise, anticipating two classes of solutions distinguished by a subscript $j=1,2$, this orthonormalization condition reads

$$\begin{aligned} a_i^*(E) a_j(E'') + \int dE' [\beta_{iE'}^*(E) \beta_{jE'}(E'') \\ + \gamma_{iE'}^*(E) \gamma_{jE'}(E'') + a_i^*(E) \beta_{jE'}(E'') S_{1E'} \\ + a_j(E'') \beta_{iE'}^*(E) S_{1E'}^* + a_i^*(E) \gamma_{jE'}(E'') S_{2E'} \\ + a_j(E'') \gamma_{iE'}^*(E) S_{2E'}^*] = \delta(E'' - E) \delta_{ij}. \end{aligned} \quad (21)$$

Since Fano's formulation assumes uncoupled continua, a prediagonalization of the interaction V_{12} between the two continua in the above model is required. This is achieved by defining two new variables associated with the continua

$$b_{E'}(E) \equiv \cos \theta \beta_{E'}(E) - \sin \theta \gamma_{E'}(E), \quad (22a)$$

$$c_{E'}(E) \equiv \sin \theta \beta_{E'}(E) + \cos \theta \gamma_{E'}(E), \quad (22b)$$

where θ is defined by

$$\begin{pmatrix} \cos \theta & -\sin \theta \\ \sin \theta & \cos \theta \end{pmatrix} \begin{pmatrix} \epsilon_1 & V_{12} \\ V_{21} & \epsilon_2 \end{pmatrix} \begin{pmatrix} \cos \theta & \sin \theta \\ -\sin \theta & \cos \theta \end{pmatrix} = \begin{pmatrix} \epsilon_- & 0 \\ 0 & \epsilon_+ \end{pmatrix}. \quad (23)$$

In terms of these variables, Eqs. (19a), (19b), and (19c) can be written as

$$\begin{aligned} \epsilon_0 a(E) + \int dE' [(v_{E'}^* - ES_{-E'}^*) b_{E'}(E) \\ + (w_{E'}^* - ES_{+E'}^*) c_{E'}(E)] = Ea(E), \end{aligned} \quad (24a)$$

$$(v_{E'} - ES_{-E'}) a(E) + (\epsilon_- + E') b_{E'}(E) = E b_{E'}(E), \quad (24b)$$

$$(w_{E'} - ES_{+E'}) a(E) + (\epsilon_+ + E') c_{E'}(E) = E c_{E'}(E), \quad (24c)$$

where

$$\begin{aligned} v_{E'} &\equiv \cos \theta V_{E'} - \sin \theta W_{E'}, & w_{E'} &\equiv \cos \theta W_{E'} + \sin \theta V_{E'}, \\ S_{-E'} &\equiv \cos \theta S_{1E'} - \sin \theta S_{2E'}, \\ S_{+E'} &\equiv \cos \theta S_{2E'} + \sin \theta S_{1E'}. \end{aligned} \quad (25)$$

The normalization condition of Eq. (20) also becomes

$$\begin{aligned} a_i^*(E) a_j(E'') + \int dE' [b_{iE'}^*(E) b_{jE'}(E'') + c_{iE'}^*(E) c_{jE'}(E'')] \\ + a_i^*(E) b_{jE'}(E'') S_{-E'} + a_j(E'') b_{iE'}^*(E) S_{-E'}^* \\ + a_i^*(E) c_{jE'}(E'') S_{+E'} + a_j(E'') c_{iE'}^*(E) S_{+E'}^* \\ = \delta(E'' - E) \delta_{ij}. \end{aligned} \quad (26)$$

It is convenient to define

$$\begin{aligned} \tilde{b}_{E'+\epsilon_-} &\equiv b_{E'}, & \tilde{c}_{E'+\epsilon_+} &\equiv c_{E'}, \\ \tilde{v}_{E'+\epsilon_-} &\equiv v_{E'}, & \tilde{w}_{E'+\epsilon_+} &\equiv w_{E'}, \\ \tilde{S}_{+,E'+\epsilon_+} &\equiv S_{+E'}, & \tilde{S}_{-,E'+\epsilon_-} &\equiv S_{-E'}, \end{aligned} \quad (27)$$

so that the system of equations (24a), (24b), and (24c) assumes the form

$$\begin{aligned} \epsilon_0 a(E) + \int dE' [(\tilde{v}_{E'}^* - E \tilde{S}_{-E'}^*) \tilde{b}_{E'}(E) + (\tilde{w}_{E'}^* - E \tilde{S}_{+E'}^*) \\ \times \tilde{c}_{E'}(E)] = Ea(E), \end{aligned} \quad (28a)$$

$$(\tilde{v}_{E'} - E \tilde{S}_{-E'}) a(E) + E' \tilde{b}_{E'}(E) = E \tilde{b}_{E'}(E), \quad (28b)$$

$$(\tilde{w}_{E'} - E \tilde{S}_{+E'}) a(E) + E' \tilde{c}_{E'}(E) = E \tilde{c}_{E'}(E). \quad (28c)$$

This is the canonical form considered by Fano, in which the bound-free couplings are corrected by a term $-E \tilde{S}_{\pm}$, due to the nonorthogonality of the basis. As shown by Fano, this system of equations admits two classes of solutions, which are given by the following: the first class is

$$a_1(E) \neq 0, \quad (29a)$$

$$\tilde{b}_{1E'}(E) = (\tilde{v}_{E'} - E \tilde{S}_{-E'}) \left\{ \frac{\mathcal{P}}{E - E'} + Z(E) \delta(E - E') \right\} a_1(E), \quad (29b)$$

$$\tilde{c}_{1E'}(E) = (\tilde{w}_{E'} - E\tilde{S}_{+E'}) \left\{ \frac{\mathcal{P}}{E-E'} + Z(E)\delta(E-E') \right\} a_1(E), \quad (29c)$$

$$\tilde{b}_{2E'}(E) = \frac{(\tilde{w}_{E'}^* - E\tilde{S}_{+E'}^*)}{(|\tilde{v}_{E'} - E\tilde{S}_{-E'}|^2 + |\tilde{w}_{E'} - E\tilde{S}_{+E'}|^2)^{1/2}} \delta(E-E'), \quad (32b)$$

where

$$Z(E) = \frac{E - \epsilon_0 - G(E)}{|\tilde{v}_E - E\tilde{S}_{-E}|^2 + |\tilde{w}_E - E\tilde{S}_{+E}|^2}, \quad (30)$$

$$G(E) \equiv \mathcal{P} \int dE' \frac{|\tilde{v}_{E'} - E\tilde{S}_{-E'}|^2 + |\tilde{w}_{E'} - E\tilde{S}_{+E'}|^2}{E-E'}. \quad (31)$$

\mathcal{P} in this last expression indicates the principal value of the integral that follows. In Eqs. (29b) and (29c), its appearance indicates formally that any integral involving $(E-E')^{-1}$ is to be understood in the sense of a principal value.

The second class is

$$a_2(E) = 0, \quad (32a) \quad \text{so that}$$

$$\tilde{c}_{2E'}(E) = \frac{-(\tilde{v}_{E'}^* - E\tilde{S}_{-E'}^*)}{(|\tilde{v}_{E'} - E\tilde{S}_{-E'}|^2 + |\tilde{w}_{E'} - E\tilde{S}_{+E'}|^2)^{1/2}} \delta(E-E'). \quad (32c)$$

The orthonormalization of the solutions within the first class according to Eq. (26) gives

$$a_1(E) = \frac{\sin \xi}{\pi(|\tilde{v}_E - E\tilde{S}_{-E}|^2 + |\tilde{w}_E - E\tilde{S}_{+E}|^2)^{1/2}}, \quad (33)$$

with

$$\xi(E) = -\arctan \left[\frac{\pi(|\tilde{v}_E - E\tilde{S}_{-E}|^2 + |\tilde{w}_E - E\tilde{S}_{+E}|^2)}{E - \epsilon_0 - G(E)} \right], \quad (34)$$

$$|a_1(E)|^2 = \frac{(|\tilde{v}_E - E\tilde{S}_{-E}|^2 + |\tilde{w}_E - E\tilde{S}_{+E}|^2)}{[E - \epsilon_0 - G(E)]^2 + \pi^2(|\tilde{v}_E - E\tilde{S}_{-E}|^2 + |\tilde{w}_E - E\tilde{S}_{+E}|^2)^2}. \quad (35)$$

This relation will be used in the following derivations of the explicit expressions of the wave packets as they are propagated in time. Within the second class, due to the fact that $a_2=0$ uniformly, the orthonormalization condition of Eq. (26) is automatically ensured. The two classes of solutions are mutually orthogonal: indeed, with $i=1$ and $j=2$, the left-hand side of Eq. (26) gives

$$-a_1^*(E)Z(E)(E-E'') \frac{\tilde{S}_{-E}(\tilde{w}_E - E\tilde{S}_{+E})^* - \tilde{S}_{+E}(\tilde{v}_E - E\tilde{S}_{-E})^*}{(|\tilde{v}_E - E\tilde{S}_{-E}|^2 + |\tilde{w}_E - E\tilde{S}_{+E}|^2)^{1/2}} \delta(E-E''),$$

which equals zero for all values of E and E'' . It is to be noted that exactly the same form of solutions are found as in Fano's original derivations, when the orthonormalization conditions of Eq. (21) or of Eq. (26) are imposed, as appropriate for a nonorthogonal basis. The only important modification to Fano's solutions for this type of problem is the correction of the bound-free couplings by the elements of the matrix $-E\tilde{S}$.

In summary, the above construction gives the following final expression for the matrix $\underline{\Omega}$ of Eqs. (16) and (18):

$$\underline{\Omega} = \underline{C}\underline{D}, \quad (36)$$

where

$$\underline{C} = \begin{pmatrix} 1 & 0 & 0 & \cdots & 0 & 0 & 0 & \cdots & 0 \\ 0 & \cos\theta & & & 0 & \sin\theta & & & 0 \\ 0 & & \cos\theta & & & & \sin\theta & & \\ \vdots & & & \ddots & & & & \ddots & \\ 0 & 0 & & & \cos\theta & 0 & & & \sin\theta \\ 0 & -\sin\theta & & & 0 & \cos\theta & & & 0 \\ 0 & & -\sin\theta & & & & \cos\theta & & \\ \vdots & & & \ddots & & & & \ddots & \\ 0 & 0 & & & -\sin\theta & 0 & & & \theta \end{pmatrix}, \quad (37)$$

symbolically represents the prediagonalization of the couplings V_{12} between the two continua associated with the two charge exchange states $1\sigma_g^{\text{H}_2^+}$, $1\sigma_u^{\text{H}_2^+}$. The matrix \underline{D} has the following form:

$$\underline{D} = \begin{pmatrix} \dots & a_k(E) & \dots & a_1(\bar{E}) & a_2(\bar{E}) & \dots \\ b_{kE_1}(E) & & & b_{1E_1}(\bar{E}) & b_{2E_1}(\bar{E}) & \\ b_{kE_2}(E) & & & b_{1E_2}(\bar{E}) & b_{2E_2}(\bar{E}) & \\ \vdots & & & \vdots & \vdots & \\ b_{kE'}(E) & & & b_{1E'}(\bar{E}) & b_{2E'}(\bar{E}) & \\ \vdots & & & \vdots & \vdots & \\ c_{kE_1}(E) & & & c_{1E_1}(\bar{E}) & c_{2E_1}(\bar{E}) & \\ \vdots & & & \vdots & \vdots & \\ c_{kE'}(E) & & & c_{1E'}(\bar{E}) & c_{2E'}(\bar{E}) & \\ \vdots & & & \vdots & \vdots & \end{pmatrix}, \quad (38)$$

with the elements $a_k(E)$, $b_{kE'}(E)$, and $c_{kE'}(E)$ given by Eqs. (29a)–(29c) and (32a)–(32c) along with the definitions of Eq. (27).

IV. WAVE-PACKET PREPARATION AND PROPAGATION

A. General structure

To implement the wave-packet propagation scheme using the split operator formula, Eq. (17), the total evolution time is divided into N small time slices $[t_n, t_{n+1}]$, $n=1, \dots, N-1$, with $t_1=0$ defining the initial moment. Consider an arbitrary time slice at the beginning of which (denoted by $t=t_0$) all channels are populated, i.e., the initial wave packets $\chi_0(R, t_0)$, $\chi_{1E'}(R, t_0)$, and $\chi_{2E'}(R, t_0)$ are all nonzero. Then, at the end of the slice, $t=t_0 + \delta t$, Eq. (17) together with Eqs. (36), (37), and (38) give

$$\begin{aligned} \chi_0(R, t_0 + \delta t) = & e^{-(i/\hbar)\hat{T}_N\delta t/2} \left\{ I_{aa} e^{-(i/\hbar)\hat{T}_N\delta t/2} \chi_0(R, t_0) + \int dE'' I_{ab}(E'') [\cos\theta e^{-(i/\hbar)\hat{T}_N\delta t/2} \chi_{1E''}(R, t_0) \right. \\ & \left. - \sin\theta e^{-(i/\hbar)\hat{T}_N\delta t/2} \chi_{2E''}(R, t_0)] + \int dE'' I_{ac}(E'') [\sin\theta e^{-(i/\hbar)\hat{T}_N\delta t/2} \chi_{1E''}(R, t_0) + \cos\theta e^{-(i/\hbar)\hat{T}_N\delta t/2} \chi_{2E''}(R, t_0)] \right\}, \end{aligned} \quad (39a)$$

$$\begin{aligned} \chi_{1E'}(R, t_0 + \delta t) = & e^{-(i/\hbar)\hat{T}_N\delta t/2} \left\{ \cos\theta \left[I_{ba}(E') e^{-(i/\hbar)\hat{T}_N\delta t/2} \chi_0(R, t_0) + \sum_k \int dE'' I_{bb}^{(k)}(E', E'') (\cos\theta e^{-(i/\hbar)\hat{T}_N\delta t/2} \chi_{1E''}(R, t_0) \right. \right. \\ & \left. \left. - \sin\theta e^{-(i/\hbar)\hat{T}_N\delta t/2} \chi_{2E''}(R, t_0) \right) + \sum_k \int dE'' I_{bc}^{(k)}(E', E'') (\sin\theta e^{-(i/\hbar)\hat{T}_N\delta t/2} \chi_{1E''}(R, t_0) \right. \\ & \left. + \cos\theta e^{-(i/\hbar)\hat{T}_N\delta t/2} \chi_{2E''}(R, t_0) \right] + \sin\theta \left[I_{ca}(E') e^{-(i/\hbar)\hat{T}_N\delta t/2} \chi_0(R, t_0) + \sum_k \int dE'' I_{cb}^{(k)}(E', E'') \right. \\ & \left. \times (\cos\theta e^{-(i/\hbar)\hat{T}_N\delta t/2} \chi_{1E''}(R, t_0) - \sin\theta e^{-(i/\hbar)\hat{T}_N\delta t/2} \chi_{2E''}(R, t_0)) + \sum_k \int dE'' I_{cc}^{(k)}(E', E'') \right. \\ & \left. \times (\sin\theta e^{-(i/\hbar)\hat{T}_N\delta t/2} \chi_{1E''}(R, t_0) + \cos\theta e^{-(i/\hbar)\hat{T}_N\delta t/2} \chi_{2E''}(R, t_0)) \right] \Big\}, \end{aligned} \quad (39b)$$

$$\begin{aligned}
\chi_{2E'}(R, t_0 + \delta t) = & e^{-(i/\hbar)\hat{T}_N\delta t/2} \left\{ -\sin\theta \left[I_{ba}(E') e^{-(i/\hbar)\hat{T}_N\delta t/2} \chi_0(R, t_0) + \sum_k \int dE'' I_{bb}^{(k)}(E', E'') \right. \right. \\
& \times (\cos\theta e^{-(i/\hbar)\hat{T}_N\delta t/2} \chi_{1E''}(R, t_0) - \sin\theta e^{-(i/\hbar)\hat{T}_N\delta t/2} \chi_{2E''}(R, t_0)) + \sum_k \int dE'' I_{bc}^{(k)}(E', E'') \\
& \times (\sin\theta e^{-(i/\hbar)\hat{T}_N\delta t/2} \chi_{1E''}(R, t_0) + \cos\theta e^{-(i/\hbar)\hat{T}_N\delta t/2} \chi_{2E''}(R, t_0)) \left. \right] + \cos\theta \left[I_{ca}(E') e^{-(i/\hbar)\hat{T}_N\delta t/2} \chi_0(R, t_0) \right. \\
& + \sum_k \int dE'' I_{cb}^{(k)}(E'', E') (\cos\theta e^{-(i/\hbar)\hat{T}_N\delta t/2} \chi_{1E''}(R, t_0) - \sin\theta e^{-(i/\hbar)\hat{T}_N\delta t/2} \chi_{2E''}(R, t_0)) \\
& \left. \left. + \sum_k \int dE'' I_{cc}^{(k)}(E', E'') (\sin\theta e^{-(i/\hbar)\hat{T}_N\delta t/2} \chi_{1E''}(R, t_0) + \cos\theta e^{-(i/\hbar)\hat{T}_N\delta t/2} \chi_{2E''}(R, t_0)) \right] \right\}, \quad (39c)
\end{aligned}$$

where

$$I_{aa}(\delta t) = \int dE |a_1(E)|^2 e^{-(i/\hbar)E\delta t}, \quad (40a)$$

$$I_{ba}(E'', \delta t) = \int dE b_{1E''}(E) a_1^*(E) e^{-(i/\hbar)E\delta t} = I_{ab}^*(E'', -\delta t), \quad (40b)$$

$$I_{ca}(E'', \delta t) = \int dE c_{1E''}(E) a_1^*(E) e^{-(i/\hbar)E\delta t} = I_{ac}^*(E'', -\delta t), \quad (40c)$$

and, for $k=1,2$

$$\begin{aligned}
I_{bc}^{(k)}(E', E'', \delta t) &= \int dE b_{kE'}(E) c_{kE''}^*(E) e^{-(i/\hbar)E\delta t} \\
&= I_{cb}^{(k)*}(E'', E', -\delta t), \quad (41a)
\end{aligned}$$

$$I_{bb}^{(k)}(E', E'') = \int dE b_{kE'}(E) b_{kE''}^*(E) e^{-(i/\hbar)E\delta t}, \quad (41b)$$

$$I_{cc}^{(k)}(E', E'') = \int dE c_{kE'}(E) c_{kE''}^*(E) e^{-(i/\hbar)E\delta t}. \quad (41c)$$

Only the energy dependence of these integrals was indicated in Eqs. (39a)–(39c) as this is more relevant than their parametric dependence on δt , which is exhibited in Eqs. (40a)–(41c) only to help highlight the symmetry of the integrals with respect to pairwise permutations of the indices $\alpha, \beta = a, b$, or c . The evaluation of these various integrals using

Eqs. (29a)–(29c), (32a)–(32c), and (27) is simplified if the bound-free coupling matrix elements depend weakly on E, E' :

$$\frac{\partial(\tilde{v}_{E'} - E\tilde{S}_{-,E'})}{\partial E} \approx 0 \approx \frac{\partial(\tilde{v}_{E'} - E\tilde{S}_{-,E'})}{\partial E'}, \quad (42)$$

$$\frac{\partial(\tilde{w}_{E'} - E\tilde{S}_{+,E'})}{\partial E} \approx 0 \approx \frac{\partial(\tilde{w}_{E'} - E\tilde{S}_{+,E'})}{\partial E'}. \quad (43)$$

These assumptions are justified for the first ionization process in consideration, for which the overlap integrals $S_{\pm, E'}$ and the matrix elements $v_{E'}, w_{E'}$ are small [35], in the relevant range of internuclear distances R , and for all values of E' lying within a neighborhood of $\epsilon_0^{\text{res}} - \epsilon_{\pm}$ of width Γ , where

$$\epsilon_0^{\text{res}} \approx \epsilon_0 + G(\epsilon_0) - i\Gamma \quad (44)$$

and

$$\begin{aligned}
\Gamma \equiv & \pi (|v_{E-\epsilon_-} - ES_{-,E-\epsilon_-}|^2 \\
& + |w_{E-\epsilon_+} - ES_{+,E-\epsilon_+}|^2) |_{E=\epsilon_0+G(\epsilon_0)} \quad (45)
\end{aligned}$$

characterize the single pole exhibited by the function $|a_1(E)|^2$, Eq. (35), in the lower complex half plane. The detailed evaluations of the above integrals under the conditions defined by Eqs. (42) and (43) and using contour integration techniques can be found in Appendix A. Using Eqs. (A5), (A12), and (A14), the above expression for the neutral molecule, ground-state channel amplitude, Eq. (39a), reduces to

$$\begin{aligned}
\chi_0(R, t_0 + \delta t) = & e^{-(i/\hbar)\hat{T}_N\delta t/2} e^{-(i/\hbar)\epsilon_0^{\text{res}}\delta t} e^{-(i/\hbar)\hat{T}_N\delta t/2} \chi_0(R, t_0) + \int dE'' e^{-(i/\hbar)\hat{T}_N\delta t/2} [v_{E''} - (E'' + \epsilon_-) S_{-E''}]^* \\
& \times F^*(-\delta t | \epsilon_0, E'' + \epsilon_-) [\cos\theta e^{-(i/\hbar)\hat{T}_N\delta t/2} \chi_{1E''}(R, t_0) - \sin\theta e^{-(i/\hbar)\hat{T}_N\delta t/2} \chi_{2E''}(R, t_0)] \\
& + \int dE'' e^{-(i/\hbar)\hat{T}_N\delta t/2} [w_{E''} - (E'' + \epsilon_+) S_{+E''}]^* F^*(-\delta t | \epsilon_0, E'' + \epsilon_+) [\sin\theta e^{-(i/\hbar)\hat{T}_N\delta t/2} \chi_{1E''}(R, t_0) \\
& + \cos\theta e^{-(i/\hbar)\hat{T}_N\delta t/2} \chi_{2E''}(R, t_0)]. \tag{46a}
\end{aligned}$$

As to the nuclear amplitudes $\chi_{kE'}$ associated with the ionic channels, it is shown in Appendix B that they reduce to

$$\begin{aligned}
\chi_{1E'}(R, t_0 + \delta t) = & \eta_{1E'}(R, t_0 + \delta t) + e^{-(i/\hbar)E'\delta t} e^{-(i/\hbar)\hat{T}_N\delta t/2} \{ \cos\theta e^{-(i/\hbar)\epsilon_- \delta t} [\cos\theta e^{-(i/\hbar)\hat{T}_N\delta t/2} \chi_{1E'}(R, t_0) \\
& - \sin\theta e^{-(i/\hbar)\hat{T}_N\delta t/2} \chi_{2E'}(R, t_0)] \} + e^{-(i/\hbar)E'\delta t} e^{-(i/\hbar)\hat{T}_N\delta t/2} \{ \sin\theta e^{-(i/\hbar)\epsilon_+ \delta t} [\sin\theta e^{-(i/\hbar)\hat{T}_N\delta t/2} \chi_{1E'}(R, t_0) \\
& + \cos\theta e^{-(i/\hbar)\hat{T}_N\delta t/2} \chi_{2E'}(R, t_0)] \} \tag{46b}
\end{aligned}$$

for the ion's σ_g state associated with an electron energy E' and

$$\begin{aligned}
\chi_{2E'}(R, t_0 + \delta t) = & \eta_{2E'}(R, t_0 + \delta t) + e^{-(i/\hbar)E'\delta t} e^{-(i/\hbar)\hat{T}_N\delta t/2} \{ -\sin\theta e^{-(i/\hbar)\epsilon_- \delta t} [\cos\theta e^{-(i/\hbar)\hat{T}_N\delta t/2} \chi_{1E'}(R, t_0) \\
& - \sin\theta e^{-(i/\hbar)\hat{T}_N\delta t/2} \chi_{2E'}(R, t_0)] \} + e^{-(i/\hbar)E'\delta t} e^{-(i/\hbar)\hat{T}_N\delta t/2} \{ \cos\theta e^{-(i/\hbar)\epsilon_+ \delta t} [\sin\theta e^{-(i/\hbar)\hat{T}_N\delta t/2} \chi_{1E'}(R, t_0) \\
& + \cos\theta e^{-(i/\hbar)\hat{T}_N\delta t/2} \chi_{2E'}(R, t_0)] \} \tag{46c}
\end{aligned}$$

for the ion's σ_u state associated with an electron energy E' .

In Eq. (46a),

$$F(\delta t | \epsilon_0, E' + \epsilon_{\pm}) \equiv \frac{\exp\{-(i/\hbar)\epsilon_0^{\text{res}}\delta t\} - \exp\{-(i/\hbar)(E' + \epsilon_{\pm})\delta t\}}{\epsilon_0^{\text{res}} - (E' + \epsilon_{\pm})} \tag{47}$$

and, in the expressions of $\chi_{kE'}$, $k=1,2$ [Eqs. (46b) and (46c)], the functions $\eta_{kE'}$ are given by

$$\begin{aligned}
\eta_{1E'}(R, t_0 + \delta t) = & e^{-(i/\hbar)\hat{T}_N\delta t/2} \{ \cos\theta [v_{E'} - (E' + \epsilon_-) S_{-E'}] F(\delta t | \epsilon_0, E' + \epsilon_-) + \sin\theta [w_{E'} - (E' + \epsilon_+) S_{+E'}] \\
& \times F(\delta t | \epsilon_0, E' + \epsilon_+) \} e^{-(i/\hbar)\hat{T}_N\delta t/2} \chi_0(R, t_0), \tag{48a}
\end{aligned}$$

$$\begin{aligned}
\eta_{2E'}(R, t_0 + \delta t) = & e^{-(i/\hbar)\hat{T}_N\delta t/2} \{ -\sin\theta [v_{E'} - (E' + \epsilon_-) S_{-E'}] F(\delta t | \epsilon_0, E' + \epsilon_-) + \cos\theta [w_{E'} - (E' + \epsilon_+) S_{+E'}] \\
& \times F(\delta t | \epsilon_0, E' + \epsilon_+) \} e^{-(i/\hbar)\hat{T}_N\delta t/2} \chi_0(R, t_0). \tag{48b}
\end{aligned}$$

Note that only the wave packet $\chi_0(R, t)$ associated with the ground state of H_2 at the previous time t_0 is involved in the composition of these functions. Thus, these functions represent the portions of $\chi_{kE'}$, $k=1,2$, that, between t_0 and $t_0 + \delta t$, are newly promoted from the ground state, and for this reason will be called source terms. In addition to these source terms, $\chi_{kE'}$, $k=1,2$ also contain terms representing the motions of previously promoted wave-packet portions on the coupled ϵ_1 and ϵ_2 surfaces. Likewise the wave packet associated with the ground channel at time $t + \delta t$ consists of a term involving $e^{-(i/\hbar)\epsilon_0^{\text{res}}\delta t}$, which, with $\epsilon_0^{\text{res}} = \epsilon_0 + G(\epsilon_0) - i\Gamma$, denotes the continuous depopulation of the ground state, and a set of terms representing the back transfer of population from the continuum of ionized channels to this state.

B. Localization of continuum wave packets: Effective five-channel scheme

A close examination of Eq. (47) shows that, due to the presence of the factor $[\epsilon_0^{\text{res}} - (E' + \epsilon_j)]^{-1}$, whose amplitude is a Lorentzian-shape function of E' localized in a neighborhood of $E' = \epsilon_0 + G(\epsilon_0) - \epsilon_j$ of width Γ , the function $F(\delta t | \epsilon_0, E' + \epsilon_j)$ is also localized in this region. As a consequence, for a given internuclear distance R , the amplitudes $\eta_{1E'}$ and $\eta_{2E'}$ acquire appreciable values in the neighborhood of two resonance energies only, namely, $E' = \Delta_-$ and $E' = \Delta_+$, where

$$\Delta_-(R) = \epsilon_0 + G(\epsilon_0) - \epsilon_-, \tag{49a}$$

$$\Delta_+(R) = \epsilon_0 + G(\epsilon_0) - \epsilon_+. \tag{49b}$$

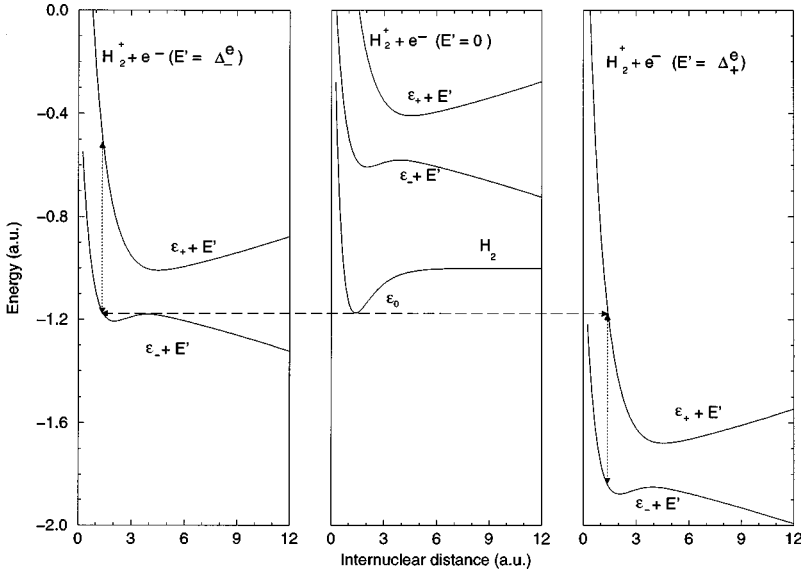


FIG. 4. Dressing of the adiabatic PES's, ϵ_- and ϵ_+ , of H_2^+ by two different energies E' of the first ionized electron, $E' = \epsilon_0^e - \epsilon_-^e = \Delta_-^e$ and $E' = \epsilon_0^e - \epsilon_+^e = \Delta_+^e$. Dashed arrows indicate bound-free couplings. Dotted arrows indicate population exchanges between the two ionic continua.

These are the energies at which the interactions of the electronic ground state of the neutral molecule with the two ionization continua are resonant. Due to the interaction V_{12} between the two continua, an interaction that was prediagonalized by the matrix \underline{C} , a resonant transfer of population from the ground manifold to one of the continua necessarily populates the other continuum so that each of the continuum amplitudes, $\eta_{1E'}$ and $\eta_{2E'}$, is localized at both resonant energy positions. This effect is illustrated schematically in Fig. 4. As R is made to vary within the spread D_0 of χ_0 , the initial vibrational state of the ground-state neutral molecule, these resonant energy positions, and the width Γ , also vary. Therefore, it is more appropriate to describe the distribution of the continuum amplitudes as being localized about resonant energy positions, $\Delta_j^e = \epsilon_0^e + G(\epsilon_0^e) - \epsilon_j^e$, $j = +, -$, defined at a fixed nuclear configuration, $R = R_e$, say, with an effective width Γ_{eff} that encompasses the spread $\delta\Delta_j$ of the resonant energies $\Delta_j = \epsilon_0 + G(\epsilon_0) - \epsilon_j$ with varying R , and can be defined by

$$\Gamma_{\text{eff}} = \max_{j=\pm} \delta\Delta_j + \Gamma, \quad (50)$$

with

$$\delta\Delta_j = \max_{R \in D_0} |\Delta_j(R)| - \min_{R \in D_0} |\Delta_j(R)|. \quad (51)$$

Since this spread is typically of the same order of magnitude as a ground-state vibrational energy difference, Γ_{eff} is expected to be much smaller than $\epsilon_+^e - \epsilon_-^e$; i.e., the two resonances can be considered well isolated from each other.

Due to their localized character, a simpler expression of the source terms, $\eta_{1E'}$ and $\eta_{2E'}$, can be obtained, for values of the ionized electron energy E' lying within the intervals $[\Delta_j^e - \Gamma_{\text{eff}}, \Delta_j^e + \Gamma_{\text{eff}}]$ by noting that for

$$\delta t \ll (\hbar/\Gamma) \quad (52)$$

it is convenient to rewrite the function $F(\delta t | \epsilon_0, E' + \epsilon_j)$ in the following way:

$$\begin{aligned} F(\delta t | \epsilon_0, E' + \epsilon_j) &= \frac{1}{2} \left\{ \frac{e^{-(i/\hbar)\epsilon_0^{\text{res}}\delta t} (1 - e^{-(i/\hbar)(E' + \epsilon_j - \epsilon_0^{\text{res}})\delta t})}{\epsilon_0^{\text{res}} - (E' + \epsilon_j)} - \frac{(1 - e^{(i/\hbar)(E' + \epsilon_j - \epsilon_0^{\text{res}})\delta t}) e^{-(i/\hbar)(E' + \epsilon_j)\delta t}}{\epsilon_0^{\text{res}} - (E' + \epsilon_j)} \right\} \\ &= \frac{1}{2} \left\{ \frac{e^{-(i/\hbar)\epsilon_0^{\text{res}}\delta t} [(i/\hbar)(E' + \epsilon_j - \epsilon_0^{\text{res}})\delta t]}{\epsilon_0^{\text{res}} - (E' + \epsilon_j)} + \frac{[(i/\hbar)(E' + \epsilon_j - \epsilon_0^{\text{res}})\delta t] e^{-(i/\hbar)(E' + \epsilon_j)\delta t}}{\epsilon_0^{\text{res}} - (E' + \epsilon_j)} \right. \\ &\quad \left. + e^{-(i/\hbar)\epsilon_0^{\text{res}}\delta t} \left[\frac{(-i/\hbar)(E' + \epsilon_j - \epsilon_0^{\text{res}})^2 \delta t^2}{\epsilon_0^{\text{res}} - (E' + \epsilon_j)} - \frac{(i/\hbar)(E' + \epsilon_j - \epsilon_0^{\text{res}})^2 \delta t^2}{\epsilon_0^{\text{res}} - (E' + \epsilon_j)} e^{-(i/\hbar)(E' + \epsilon_j - \epsilon_0^{\text{res}})\delta t} \right] \right\} + O(\delta t^3), \end{aligned}$$

ielding

$$F(\delta t|\epsilon_0, E' + \epsilon_j) = -\frac{i}{\hbar} \delta t (e^{-(i/\hbar)\epsilon_0^{\text{res}} \delta t} + e^{-(i/\hbar)(E' + \epsilon_j) \delta t}) \times \Theta(E' - \Delta_j|\Gamma), \quad (55)$$

$$+ O(\delta t^3) \quad (53)$$

for all $E' \in [\epsilon_0 + G(\epsilon_0) - \epsilon_j - \Gamma, \epsilon_0 + G(\epsilon_0) - \epsilon_j + \Gamma]$, while F is virtually zero outside this interval. Introducing

$$\Theta(x|\alpha) \equiv \begin{cases} 1, & x \in [-\alpha, \alpha] \\ 0, & x \notin [-\alpha, \alpha] \end{cases} \quad (54)$$

the function $F(\delta t|\epsilon_0, E' + \epsilon_j)$ can thus be rewritten in the form

given that the time scale over which the split-operator formula, Eq. (15), is convergent certainly satisfies Eq. (52). In the light of the above discussion concerning the variation of the Feschbach resonances' positions and widths with R , the above expression of the function F , Eq. (55), can be modified by replacing $\Delta_j(R)$ by Δ_j^e and the R -dependent width Γ by Γ_{eff} . Then, Eqs. (48a) and (48b) can be written as

$$\eta_{1E'}(R, t_0 + \delta t) = -i \frac{\delta t}{2\hbar} e^{-(i/\hbar)\hat{T}_N \delta t/2} \{ [v_{E'} - (E' + \epsilon_-) S_{-E'}] \cos\theta [e^{-(i/\hbar)\epsilon_0^{\text{res}} \delta t} + e^{-(i/\hbar)(E' + \epsilon_-) \delta t}] \Theta(E' - \Delta_-^e|\Gamma_{\text{eff}}) + [w_{E'} - (E' + \epsilon_+) S_{+E'}] \sin\theta [e^{-(i/\hbar)\epsilon_0^{\text{res}} \delta t} + e^{-(i/\hbar)(E' + \epsilon_+) \delta t}] \Theta(E' - \Delta_+^e|\Gamma_{\text{eff}}) \} e^{-(i/\hbar)\hat{T}_N \delta t/2} \chi_0(R, t_0) + O(\delta t^3), \quad (56a)$$

$$\eta_{2E'}(R, t_0 + \delta t) = -i \frac{\delta t}{2\hbar} e^{-(i/\hbar)\hat{T}_N \delta t/2} \{ -[v_{E'} - (E' + \epsilon_-) S_{-E'}] \sin\theta [e^{-(i/\hbar)\epsilon_0^{\text{res}} \delta t} + e^{-(i/\hbar)(E' + \epsilon_-) \delta t}] \Theta(E' - \Delta_-^e|\Gamma_{\text{eff}}) + [w_{E'} - (E' + \epsilon_+) S_{+E'}] \cos\theta [e^{-(i/\hbar)\epsilon_0^{\text{res}} \delta t} + e^{-(i/\hbar)(E' + \epsilon_+) \delta t}] \Theta(E' - \Delta_+^e|\Gamma_{\text{eff}}) \} e^{-(i/\hbar)\hat{T}_N \delta t/2} \chi_0(R, t_0) + O(\delta t^3). \quad (56b)$$

Given the localization of these source terms, as described by the Θ factor, the variable E' in $[v_{E'} - (E' + \epsilon_-) S_{-E'}]$ and $[w_{E'} - (E' + \epsilon_+) S_{+E'}]$ in Eqs. (56a) and (56b) may be replaced by Δ_j^e , $j = -$ or $+$, and $\epsilon_0^{\text{res}} = \epsilon_0 + G(\epsilon_0) - i\Gamma$ in the $\exp\{-i/\hbar\epsilon_0^{\text{res}} \delta t\}$ factor may be replaced by $E' + \epsilon_j - i\Gamma$. This gives, up to order δt^3 ,

$$\eta_{1E'}(R, t_0 + \delta t) \approx e^{-(i/\hbar)E' \delta t} \{ \Theta(E' - \Delta_-^e|\Gamma_{\text{eff}}) \eta_{1-}^-(R, t_0 + \delta t) + \Theta(E' - \Delta_+^e|\Gamma_{\text{eff}}) \eta_{1+}^+(R, t_0 + \delta t) \}, \quad (57a)$$

$$\eta_{2E'}(R, t_0 + \delta t) \approx e^{-(i/\hbar)E' \delta t} \{ \Theta(E' - \Delta_-^e|\Gamma_{\text{eff}}) \eta_{2-}^-(R, t_0 + \delta t) + \Theta(E' - \Delta_+^e|\Gamma_{\text{eff}}) \eta_{2+}^+(R, t_0 + \delta t) \}, \quad (57b)$$

with

$$\eta_{1(2)-}^-(R, t_0 + \delta t) = i \frac{\delta t}{2\hbar} e^{-(i/\hbar)\hat{T}_N \delta t/2} [v_{E'} - (E' + \epsilon_-) S_{-E'}] |_{E' = \Delta_-^e} \begin{pmatrix} \cos\theta \\ -\sin\theta \end{pmatrix} (e^{-(\Gamma/\hbar)\delta t} + 1) e^{-(i/\hbar)\epsilon_- \delta t} e^{-(i/\hbar)\hat{T}_N \delta t/2} \chi_0(R, t_0), \quad (58a)$$

$$\eta_{1(2)+}^+(R, t_0 + \delta t) = i \frac{\delta t}{2\hbar} e^{-(i/\hbar)\hat{T}_N \delta t/2} [w_{E'} - (E' + \epsilon_+) S_{+E'}] |_{E' = \Delta_+^e} \begin{pmatrix} \sin\theta \\ \cos \end{pmatrix} (e^{-\Gamma/\hbar \delta t} + 1) e^{-(i/\hbar)\epsilon_+ \delta t} e^{-(i/\hbar)\hat{T}_N \delta t/2} \chi_0(R, t_0). \quad (58b)$$

A noteworthy feature of the final expression, Eqs. (57a) and (57b) of the source terms $\eta_{kE'}$, $k = 1, 2$, is the separation of the E' and R variables. Within each energy band centered at a resonance energy Δ_{\pm}^e , the various $\eta_{kE'}$, corresponding to different values of E' , depend on E' only through a separate phase factor $\exp\{-i/\hbar E' \delta t\}$, and share the same R dependence described by the function $\eta_k^{\pm}(R, t)$. It turns out that this type of factorization characterizes the wave packets $\chi_{kE'}$ at all times if the initial conditions correspond to the experimental situation, i.e., if $\chi_{kE'}(R, 0) = 0$, for all E' and $k = 1, 2$, while $\chi_0(R, 0) = \psi_v^0(R)$, a vibrational eigenstate of the neutral molecule ground state. To see this, note first that this factorization certainly holds at $t = \delta t$, i.e., at the end of the first time slice since with the above initial condition $\chi_{kE'} = \eta_{kE'}$ at this time. It suffices then to show that if this factorization holds at $t = t_0$, then it also holds at $t = t_0 + \delta t$. Indeed substituting the form assumed for $\chi_{kE'}(R, t_0)$,

$$\chi_{1(2)E'}(R, t_0) = e^{-(i/\hbar)E' t_0} \{ \Theta(E' - \Delta_-^e|\Gamma_{\text{eff}}) \chi_{1(2)-}^-(R, t_0) + \Theta(E' - \Delta_+^e|\Gamma_{\text{eff}}) \chi_{1(2)+}^+(R, t_0) \}, \quad (59)$$

into Eqs. (46a), (46b), and (46c), and carrying out the prescribed integrations over E'' within the same approximations as in Eqs. (42) and (43), the following final expressions are obtained:

$$\chi_0(R, t_0 + \delta t) = e^{-(i/\hbar)\hat{T}_N\delta t/2} e^{-(i/\hbar)[\epsilon_0 + G(\epsilon_0) - i\Gamma]\delta t} e^{-(i/\hbar)\hat{T}_N\delta t/2} \chi_0(R, t_0), \quad (60a)$$

$$\chi_{1(2)E'}(R, t_0 + \delta t) = e^{-(i/\hbar)E'(t_0 + \delta t)} \{ \Theta(E' - \Delta_-^e |\Gamma_{\text{eff}}|) \chi_{1(2)}^-(R, t_0 + \delta t) + \Theta(E' - \Delta_+^e |\Gamma_{\text{eff}}|) \chi_{1(2)}^+(R, t_0 + \delta t) \}, \quad (60b)$$

where the $\chi_k^\pm(R, t_0 + \delta t)$'s are

$$\begin{aligned} \begin{pmatrix} \chi_1^\pm(R, t_0 + \delta t) \\ \chi_2^\pm(R, t_0 + \delta t) \end{pmatrix} &= e^{i\Delta_\pm^e t_0/\hbar} \begin{pmatrix} \eta_1^\pm(R, t_0 + \delta t) \\ \eta_2^\pm(R, t_0 + \delta t) \end{pmatrix} + \exp\left\{ -\frac{i}{\hbar} \hat{T}_N \frac{\delta t}{2} \right\} \begin{pmatrix} \cos\theta & \sin\theta \\ -\sin\theta & \cos\theta \end{pmatrix} \begin{pmatrix} e^{-(i/\hbar)\epsilon_- \delta t} & 0 \\ 0 & e^{-(i/\hbar)\epsilon_+ \delta t} \end{pmatrix} \\ &\times \begin{pmatrix} \cos\theta & -\sin\theta \\ \sin\theta & \cos\theta \end{pmatrix} \exp\left\{ -\frac{i}{\hbar} \hat{T}_N \frac{\delta t}{2} \right\} \begin{pmatrix} \chi_1^\pm(R, t_0) \\ \chi_2^\pm(R, t_0) \end{pmatrix}, \end{aligned} \quad (61)$$

with initial conditions given by $\chi_k^\pm(R, 0) = 0$, $k = 1, 2$.

Equation (60b) confirms that the factorized structure of the ionized continuum amplitudes is preserved at all times so that the original problem, which involves an infinite number of coupled channels, is reduced to an effective five-channel problem: only five functions χ_0 , χ_1^\pm , and χ_2^\pm defined recursively by Eqs. (60a)–(61) need be calculated to obtain the full wave-packet description of the system during any stage of the ionization process. Within each ionized-electron energy band, the spatial factor χ_k^\pm of $\chi_{kE'}$ given by Eq. (61) consists of two terms: the source term η^\pm analyzed above and a term denoting the further propagation of the previously promoted part of the continuum wave packets on the ionized state PES's. Note that the final expression for χ_0 no longer contains a set of terms denoting the back transfer of population from the ionized continuum to the neutral ground state; in the approximations made here, Eqs. (42) and (43), the ground-state population is transferred irreversibly to the ionized continuum. In the context of this wave-packet propagation scheme for the nuclear dynamics accompanying a tunnel ionization process, the reduction of the problem to an effective five-channel problem reflects the well-known on-the-energy shell transition hypothesis originally introduced by Fano, which rests upon the same kind of approximations made here, Eqs. (42) and (43). Insofar as the bound-free coupling matrix elements are weak as is the case for the first ionization of H₂ in the neighborhood of the neutral ground-state equilibrium geometry [35], this hypothesis of on-the-energy shell transition is well justified and the wave-packet dynamics are accurately represented by the above recurrence formulas, Eqs. (60a), (60b), and (61).

V. NUMERICAL CALCULATIONS

A. Algorithm

With the above results, the wave-packet description of the tunnel ionization of H₂ has become completely tractable. Eqs. (60a) and (60b) used recursively together with Eqs. (61) and Eqs. (58a) and (58b) give an algorithm for the numerical wave-packet preparation and propagation during the continuous tunnel ionization of H₂. As mentioned previously, the total duration of the laser pulse is divided into short time slices $[t_n, t_{n+1}]$ with $t_n = (n-1)\delta t$ so that $t_1 = 0$ corre-

sponds to the beginning of the laser pulse. At this initial moment, only the neutral molecule ground state, i.e., ϵ_0 , is populated and $\chi_0(R, 0)$ is the vibrational eigenfunction $v = 0$ of H₂, while $\chi_{kE'}(R, 0)$ are identically zero. Eqs. (60a), (60b), (61), (58a), and (58b) evaluated with $t_0 = t_1 = 0$ then give the wave packet at $t = \delta t = t_2$, i.e., at the beginning of the second time slice. These are used in the next cycle to give χ_0 , χ_k^\pm , hence $\chi_{kE'}$, at $t = t_3$. This is repeated until the laser pulse is over.

Results reported below pertaining to the study of step 2 alone in Fig. 1 are obtained by wave-packet propagation on the two coupled manifolds of the ionic species only. In this case, the initial wave packet is the $v = 0$ vibrational state of the ground-state neutral species, considered to be vertically promoted on the $^2\Sigma_g^+$ ground manifold of H₂⁺ at time $t = 0$. This simpler wave-packet propagation study employs the usual implementation of the split-operator formula for two coupled channels.

At all stages of any wave-packet propagation procedure, the actions of the exponential operators involving the nuclear kinetic energy are evaluated in the momentum representation while those of the operators that depend only on the potential matrix elements are evaluated in the coordinate representation. Passage from the coordinate representation to the momentum representation is achieved using a fast Fourier transform procedure.

When the wave-packet propagation is carried out over a time that is long as compared to the typical time scale for large amplitude nuclear motions in the coupled channels of the ionized species, wave-packet extension over a large region of space may require an unpractically large spatial grid. To avoid this, a procedure is employed to split the excited manifold's wave functions χ_k^\pm (or χ_k simply, in the study of step 2 alone), $k = 1, 2$, into two parts: an outer part defined over the asymptotic region of the ionized state PES's ϵ_1 and ϵ_2 , where the contributions of the source terms η_k^\pm are zero, and an inner part associated with the region of space where the Hellmann-Feynman forces derived from the PES's are nonzero and where the wave packets χ_k^\pm are numerically composed and propagated by actually using Eqs. (61). In the outer region, the asymptotic laser-driven dynamics of the wave packets χ_k^\pm can be related to an equivalent laser-driven free-particle dynamics problem and can be described analyti-

TABLE I. Molecular parameters used for the evaluation of potential-energy surfaces and transition moment in H_2 and H_2^+ .

Potential	D_0 (eV)	β (a_0^{-1})	R_e (a_0)	t	A (eV)
$\epsilon_0(R)$	4.7484	1.03	1.4	1.0	13.606
$\epsilon_1(R)$	2.7925	0.72	2.0	1.0	0
$\epsilon_2(R)$	2.7925	0.72	2.0	-1.11	0
Transition moment		μ (ea_0)	μ' (e)	y	
$V_{12}(R)$		1.07	0.396	-0.055	

cally. This splitting procedure that permits the analytical propagation of asymptotic wave packets was originally developed by Heather and Metiu [36] and later adapted by Keller [37] to the case of H_2^+ , where the asymptotic wave packets are coupled together by a linear transition dipole moment. It is used here to circumvent the need to use an impractical, large spatial grid that would otherwise be required to represent the large-amplitude wave-packet motions and also to obtain the kinetic energy distribution of dissociated fragments. To this end, a relative momentum distribution is extracted from the Fourier transforms of the asymptotic parts of the wave packets and is then converted to an equivalent normalized distribution for the kinetic energy of a single H^+ fragment viewed in the center-of-mass frame.

B. Computational details

1. Model parameters

The one-dimensional potential-energy surfaces for the rotationless neutral molecule $X^1\Sigma_g^+$ ground state and the ionized molecule $^2\Sigma_g^+$, $^2\Sigma_u^+$ states are modeled by Morse functions [38]

$$\epsilon_i(R) = D_0 \{ \exp[-2\beta_i(R - R_{e_i})] - 2t_i \exp[-\beta_i(R - R_{e_i})] \} - A_i \quad (i=0, 1, \text{ or } 2) \quad (62)$$

and the transition dipole moment between the two states of H_2^+ is modeled by

$$\mu_{12}(R) = \begin{cases} \mu + (\mu'/\beta y) \{ 1 - \exp[-\beta y(R - R_e)] \} & \text{for } R \leq 12 \text{ a.u.} \\ R/2 & \text{for } R > 12 \text{ a.u.} \end{cases} \quad (63)$$

The laser field $\vec{\mathcal{E}}(t)$ yields an interaction between the two states that is given by

$$V_{12} = \vec{\mu}_{12} \cdot \vec{\mathcal{E}}(t). \quad (64)$$

The relevant parameters defining $\epsilon_0, \epsilon_1, \epsilon_2$ according to Eq. (62) and μ_{12} according to Eq. (63) are given in Table I. The laser electric field $\vec{\mathcal{E}}(t)$ is polarized along the internuclear axis and its amplitude is given by

$$\mathcal{E}(t) = f(t) \cos(\omega t + \delta), \quad (65)$$

where $\omega = 2\pi/T_L$, $T_L = 35.65$ fs, corresponding to a carrier wavelength of $10.6 \mu\text{m}$. In the full calculations including the first ionization step, the phase shift δ in this expression is zero, and the envelope function $f(t)$ is given by

$$f(t) = \begin{cases} \mathcal{E}_0 e^{-(t-t_{\text{rise}})^2} & \text{for } t \leq t_{\text{rise}} \\ \mathcal{E}_0 & \text{for } t_{\text{rise}} < t \leq 20T_L \\ \mathcal{E}_0 e^{-(t-20T_L-t_{\text{rise}})^2} & \text{for } 20T_L < t \leq t_{\text{end}} \end{cases}, \quad (66)$$

with $t_{\text{rise}} = 7$ fs. In the study of step 2 alone where the wave-packet propagation is restricted to the two electronic manifolds of H_2^+ , $f(t)$ is considered constant, $f(t) = \mathcal{E}_0$ for all t , and various values of the phase shift δ correspond to different delays in time between the moment the initial wave packet is prepared on the $^2\Sigma_g^+$ surface, and the onset of the field. For example, with $\delta = 0$, the initial wave-packet preparation occurs at peak intensity, whereas with $\delta = \pi/2$, it occurs when the field is zero. This procedure was initially used to demonstrate the sensitivity of the wave-packet dynamics during step 2 with respect to the initial conditions. A fixed value for the amplitude \mathcal{E}_0 is used in all the calculations reported below and corresponds to a fixed value of the field intensity, $I = 5 \times 10^{13} \text{ W/cm}^2$. The matrix elements $v_{E'} - (E' + \epsilon_-)S_{-E'}$ and $w_{E'} - (E' + \epsilon_+)S_{+E'}$ defining the bound-free coupling in the present Feshbach model for the tunnel ionization of H_2 are evaluated on the corresponding energy shell. Thus $E' = \Delta_-^e$ for $v_{E'} - (E' + \epsilon_-)S_{-E'}$, while $E' = \Delta_+^e$ for $w_{E'} - (E' + \epsilon_+)S_{+E'}$, and $v_{E'}$ and $w_{E'}$ are given by Eqs. (25). The determination of these matrix elements requires the calculation of matrix elements of the single electron dipole moment operator \vec{r} between the $1\sigma_g^{\text{H}_2}$ orbital of H_2 and the ionized electron wave function \mathcal{A}_E or the $1\sigma_g^{\text{H}_2^+}$ of H_2^+ ; see Eqs. (13a) and (13b). Using the well-known minimal basis expression of the orbitals and the Airy approximation to the time-dependent wave function \mathcal{A}_E , these matrix elements, as well as the overlap integrals $\langle 1\sigma_g^{\text{H}_2} | \mathcal{A}_E \rangle$, are calculated by numerical integration; the integrals are restricted to the electronic dimension parallel to the field polarization. Because of the restriction of these integrals to this single dimension and the use of the simple Airy function to represent \mathcal{A}_E , which, more correctly, should be constructed as Airy-Coulomb waves, the amplitude of the bound-free coupling matrix elements is underestimated, yielding ionization rates that are lower than predicted by the standard ADK expression for vertical static tunnel ionization [14,39]. Figure 5 compares the vertical ionization rate W_{ion} associated with the present formalism with the rate $W_{\text{ion}}^{\text{ADK}}$ predicted by ADK theory as a function of the field intensity. Within the present formalism, this rate is estimated by

$$W_{\text{ion}}(I) = \frac{1}{T_L} \left(1 - \exp \left[- \int_0^{T_L} dt' \Gamma^e(t') \right] \right),$$

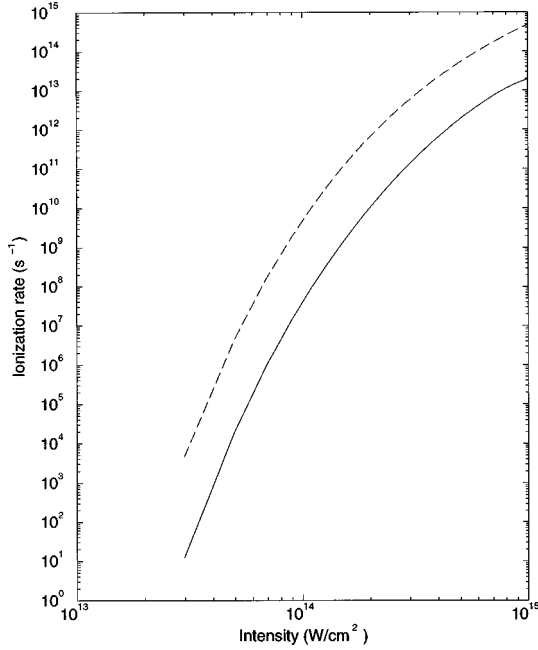


FIG. 5. Ionization rates of H₂ as a function of the field intensity, calculated using the present formalism (solid line) and the ADK theory (dashed line). The rates are evaluated at the equilibrium internuclear distance and the field has a wavelength of 10.6 μm .

where $\Gamma^e(t')$ is the instantaneous width defined by Eq. (45) at $R=R_e$. It is seen that a correct intensity dependence is obtained but W_{ion} and $W_{\text{ion}}^{\text{ADK}}$ differ by an order of magnitude. This reflects the approximations made in the evaluation of the bound-free coupling matrix elements as detailed above. However, the phases of the wave packets continuously promoted on the excited channels by tunnel ionization are expected to be weakly affected by these approximations as can be seen by analyzing the structures of the recurrence formulas of Eqs. (60a), (60b), and (61). Insofar as the main object of our study is the effect that the continuous tunnel ionization can have on the wave-packet dynamics, the errors made in estimating the amplitude of the bound-free matrix elements are inconsequential. In principle, as \mathcal{A}_E varies with time and R , the bound-free coupling matrix elements must be recalculated at each time step. These calculations thus constitute the time-consuming part of the entire wave-packet propagation scheme.

2. Temporal and spatial grids

The time step δt onto which the total evolution time must be divided is governed by the smallest of the two natural time scales of the problem: the typical vibrational period of H₂⁺ and the period of the field. The latter is important since a quasistatic picture is implicit in the construction of the basis \mathcal{B} of Eq. (6). Thus δt must be such that the amplitude of the laser electric field varies little on this time scale. With $\delta t=0.05$ fs, this condition is well satisfied and the laser pulsewidth encompasses more than 20 000 time steps.

The wave packet χ_0 and the internal parts of the components χ_1^\pm , χ_2^\pm are discretized on a spatial grid containing 1024 points covering the interval $[0, R_{\text{max}}]$ with $R_{\text{max}}=30$ \AA ; thus the spatial grid size is $\delta R=2.93 \times 10^{-2}$ \AA and that of the corresponding grid in the reciprocal momentum

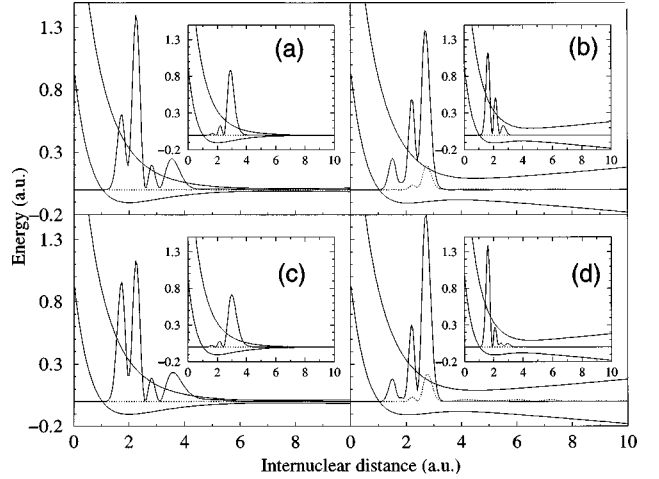


FIG. 6. Nuclear probability distributions associated with the wave packets χ_- (solid line) and χ_+ (dashed line) supported by the adiabatic channels ϵ_- and ϵ_+ for a value $E'=\Delta_-^e$ of the ionized electron energy. These wave packets are taken at four times within the 19th optical cycle: (a) $t=19\frac{1}{4}T_L$, (b) $t=19\frac{1}{2}T_L$, (c) $t=19\frac{3}{4}T_L$, (d) $t=20T_L$. The insets show the corresponding results obtained in the study of step 2 alone at these times. The initial wave function used in the insets corresponds to the $v=0$ vibrational state of the electronic ground state of H₂. This initial wave function is instantly promoted on the ground ionic channel when the field is at its peak intensity; this corresponds to $\delta=0$ in Eq. (65).

space is $\delta P/\hbar=2.09 \times 10^{-1}$ \AA^{-1} . For the numerical calculation of the one-dimensional electronic integrals needed in forming the bound-free ‘‘on-the-energy-shell’’ matrix elements $v_{E'}-(E'+\epsilon_-)S_{-E'}$ and $w_{E'}-(E'+\epsilon_+)S_{+E'}$, a grid containing 800 points and extending from $z=-4.232$ \AA to $z=4.232$ \AA is used. Since the wave function χ_0 is peaked at the equilibrium internuclear distance of the neutral molecule, $R=0.79$ \AA , and since its spatial range remains smaller than 1 \AA at all times, the matrix elements $v_{E'}-(E'+\epsilon_-)S_{-E'}$ and $w_{E'}-(E'+\epsilon_+)S_{+E'}$ were not evaluated for R larger than 6.348 \AA .

C. Results

To discuss the results of the wave-packet propagations using the present algorithm, which allows for the complete inclusion of the tunnel ionization step, it is useful to show these results in parallel with those of the separate, strictly two-state study of the second step of Fig. 1. Figure 6 shows the wave packets associated with the adiabatic channels ϵ_\pm of the ionized H₂⁺ species for a value $E'=\Delta_-^e$ of the ionized electron energy. Wave packets associated with the higher-energy band, $E' \simeq \Delta_+^e$, are found to be of much smaller amplitudes. The wave packets of Fig. 6 are taken at four typical phases of the field oscillations within the 19th optical cycle. To facilitate viewing them together with the adiabatic potential changes, these wave packets have been renormalized to the total ionized-state population. Also reproduced in the insets, to be found in each panel of this figure, are (evaluated at the same moments of time) the wave packets that were obtained in the study of step 2 alone for $\delta=0$ in Eq. (65). Recall that these evolved from the same initial wave function described above, denoting the ground vibrational state of the

neutral parent. However, here, this initial wave packet is considered to be instantly promoted on the ground ionic channel as the field is at its peak intensity. The results of the full calculations, where the continuous tunnel ionization is properly included, indicate a pronounced nonadiabatic character of the wave-packet dynamics, while these dynamics are adiabatic in the study of step 2 alone. Indeed, in this study of step 2 alone, a single wave packet is associated with the lower adiabatic channel at all times. In fact, this is the case for all other values of δ considered. In contrast, the present complete calculations show that the upper channel is occasionally populated. If the dynamics were adiabatic, then any wave-packet portion previously promoted on this channel would stay on this channel forever. The periodic disappearance of the wave packet associated with the upper adiabatic PES indicates that an appreciable nonadiabatic population transfer occurs between the two adiabatic states of the ion. It is also interesting to note that the centers of the wave packets exhibit dynamics that are synchronized with the field oscillations in a manner that is opposite to what is observed in the case of the step 2 alone with $\delta=0$. While the motions of the wave packets shown in the insets are synchronized such that only small portions of the wave packets can escape from the potential well of the lower adiabatic channel, the wave-packet dynamics observed in the complete calculation (step 1+step 2) appear to offer more favorable conditions for the dissociation of the ion. Whether this is actually the case or not will become clear in the further discussion to be found below.

Figure 7 shows, as a function of time, the total population associated with the bound vibrational states $|v(\text{H}_2^+)\rangle$ of the ionic species. In panel (a), this population is shown in absolute form and is given by

$$P_{\text{bound}}^{\text{abs}}(t) = \sum_v |\langle v(\text{H}_2^+) | \chi_1(t) \rangle|^2. \quad (67)$$

It is, however, more instructive and meaningful to consider a bound-state population P_{bound} renormalized to the total population of the ionic states. This is shown in the panel (b) of Fig. 7, and is defined by

$$P_{\text{bound}}(t) = \frac{\sum_v |\langle v(\text{H}_2^+) | \chi_1(t) \rangle|^2}{\langle \chi_1(t) | \chi_1(t) \rangle + \langle \chi_2(t) | \chi_2(t) \rangle}. \quad (68)$$

In the above definitions, the wave packets χ_1 and χ_2 are supported by the two charge-resonant states of the ion associated with a given value of the ionized electron energy, and the vibrational states $|v(\text{H}_2^+)\rangle$ are defined as the bound eigenstates of the Morse oscillator associated with the ground state of the ion, Eq. (62). In the study of step 2 alone, there is no distinction between P_{bound} and $P_{\text{bound}}^{\text{abs}}$ since then, $\langle \chi_1(t) | \chi_1(t) \rangle + \langle \chi_2(t) | \chi_2(t) \rangle = 1$. In contrast, in the complete study, the total conserved population includes that of the neutral species' ground state. Thus, in this case, the complement of the relative bound-state population P_{bound} represents the probability that the ion is in a dissociative continuum whereas the complement of $P_{\text{bound}}^{\text{abs}}$ is dominated by the neutral ground-state population. For this reason, it is more meaningful to analyze P_{bound} than $P_{\text{bound}}^{\text{abs}}$ although the former is not defined at $t=0$ when the ionic state populations

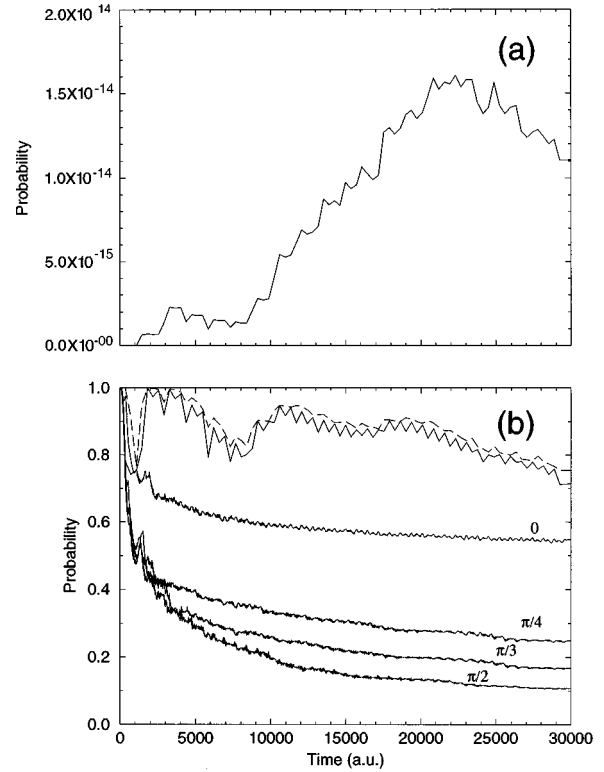


FIG. 7. (a) Absolute total population, $P_{\text{bound}}^{\text{abs}}$, associated with the vibrational states of H_2^+ . (b) Renormalized total population P_{bound} associated with the vibrational states of H_2^+ (solid line) and localized population P_{loc} (dashed line). This results for P_{bound} from the study of step 2 alone are reproduced for four values of the phase shift δ in Eq. (65), $\delta=0, \pi/4, \pi/3,$ and $\pi/2$.

are zero, and may be somewhat misleading as it appears to start from an unphysical value close to unity: in this respect, it is important to keep in mind that P_{bound} is the probability that the ion, *once formed*, stays within the manifold of its field-free vibrational bound states.

Also shown in Fig. 7(b) (dashed line) is a localized population defined by

$$P_{\text{loc}}(t) = \frac{\int_0^{R_{\text{end}}} |\chi_1(R, t)|^2 dR}{\langle \chi_1(t) | \chi_1(t) \rangle + \langle \chi_2(t) | \chi_2(t) \rangle}, \quad (69)$$

where $R_{\text{end}}=12$ a.u. so that the range of the integral in Eq. (69) encompasses the supports of all the bound vibrational states. For comparison, a set of corresponding $P_{\text{bound}}(t)$ results obtained in the two-state, study of step 2 alone with $\delta=0, \pi/4, \pi/3,$ and $\pi/2$ is shown in the same panel of Fig. 7. In this case, the graph of P_{bound} exhibits two distinct decay regimes: an initial fast decay occurring within a few optical cycles of the IR laser field, followed by a much slower decay, which, for the same pulse duration, leads to a final plateau in the bound-state population ranging from 16% for a phase shift $\delta=\pi/2$ to 65% for a zero phase shift. In the case of $\delta=0$, the synchronization between the field oscillations, which govern the time variation of the adiabatic potentials ϵ_+, ϵ_- , and the nuclear motion is such as to give the largest bound components in the wave packet χ_1 . This denotes an important stabilization of the ion with respect to dissociation. With the tunnel ionization operating continuously, the

bound-state population tends to remain larger at all times, attaining a final value exceeding 70% at the end of the pulse. This appears to be most surprising since the observations concerning the synchronization of the wave-packet dynamics with respect to the field oscillations, made above, suggest the contrary, i.e., that the ion would be less stabilized. However, the observed higher plateau in P_{bound} can be partially understood by noting that the continuous tunnel ionization tends to create, at the beginning of each time slice, new wave-packet components that are localized in the internal region associated with the bound states. Note that P_{bound} exhibits oscillations that are in-phase with those of the field and that, when the field attains its peak intensity, P_{bound} and P_{loc} are equal and P_{bound} is at a local maximum, which agrees with the above interpretation. The oscillations in P_{bound} are also observed in the case of step 2 alone. However, in the case of the complete study, including continuous ionization, they are much more pronounced and are characterized by dips that are particularly pronounced during the first optical cycles. These reflect the fast, initial decay regime, which is clearly delineated in the two-state results of step 2 alone and is here quickly compensated for by the continuous population transfer from the neutral ground state. The dips come from the repetition of this decay after each population burst (maxima in P_{bound}) occurring at peak intensity. On the other hand, the localized population varies more smoothly and the dips it exhibits at short times are much shallower than those of the bound-state population. This indicates that the wave packets contain a part lying in the dissociative continua of the two-state ionic species and that is nevertheless localized within the range of the attractive ground-state potential at all times. Does this effect occur concomitantly with a larger dissociation probability of the ion as suggested at first sight by the wave-packet dynamics shown in Fig. 6? In this respect, it is interesting to note that if one follows closely the wave-packet portions found, in the full calculation, in the vicinity of the potential gap when this is widely opened at those moments the field amplitude is at a maximum, then it turns out that these wave-packet portions tend to be reflected back towards the inner region at a later time instead of proceeding towards the dissociative limit. This is seen by comparing Fig. 6(b) to Fig. 6(c). However, it is hazardous to assess in this manner the dissociative or nondissociative character of the wave packets obtained in the presence of continuous ionization as compared to those observed in the study of step 2 alone, precisely because the continuous ionization always gives a bias towards a much larger nondissociative population. A reliable, unbiased assessment of the dissociation rate in the presence of the continuous ionization can be obtained by measuring the slopes of the dips exhibited in P_{bound} or P_{loc} after each maximum reached in Fig. 7(b), as these slopes furnish upper and lower bounds for the dissociation rate. This can be seen by invoking the following *phenomenological* rate equations:

$$\frac{dP_{\text{loc}}}{dt} = -v^{\text{diss}}(t) + v^{\text{loc}}(t), \quad (70a)$$

$$\frac{dP_{\text{bound}}}{dt} = -v^{\text{diss}}(t) + v^{\text{loc}}(t) + v^{\text{tr}}(t), \quad (70b)$$

where $v^{\text{diss}}(t)$ is the proper rate of dissociation of H₂⁺, $v^{\text{loc}}(t)$ represents the rate of change in the localized population (normalized to the total ionic population), a change that accounts for the continuous ionization of H₂, and $v^{\text{tr}}(t)$ represents the rate of population transfer between the bound states and the dissociative continuum. This last quantity, $v^{\text{tr}}(t)$, is positive when the transfer is from the continuum states to the bound states and negative for a transfer in the opposite direction. On the other hand, by definition, v^{diss} and v^{loc} are always positive. Hence, Eq. (70a) implies

$$-\frac{dP_{\text{loc}}}{dt} \leq v^{\text{diss}}(t) \quad (71)$$

for all t . At a time $t = \bar{t}_n$ lying within the time interval associated with one of the dips exhibited both by P_{bound} and P_{loc} in Fig. 7(b), localized population is being transferred from the bound states to the dissociation continuum, so that

$$v^{\text{tr}} \leq 0. \quad (72)$$

Furthermore, if \bar{t}_n is chosen such that [40]

$$v^{\text{loc}}(\bar{t}_n) = 0 \quad (73a)$$

or, less stringently, such that

$$v^{\text{loc}}(\bar{t}_n) < |v^{\text{tr}}(\bar{t}_n)| \quad (73b)$$

then (70b) gives

$$-\left. \frac{dP_{\text{bound}}}{dt} \right|_{\bar{t}_n} = v^{\text{diss}}(\bar{t}_n) - [v^{\text{tr}}(\bar{t}_n) + v^{\text{loc}}(\bar{t}_n)] \geq v^{\text{diss}}(\bar{t}_n). \quad (74)$$

Thus, the slopes of the dips exhibited by P_{loc} and P_{bound} in Fig. 7(b) provide upper and lower bounds for the dissociation rate $v^{\text{diss}}(\bar{t}_n)$ evaluated right after each burst in the population of the ionic channels

$$-\left. \frac{dP_{\text{loc}}}{dt} \right|_{\bar{t}_n} \leq v^{\text{diss}}(\bar{t}_n) \leq -\left. \frac{dP_{\text{bound}}}{dt} \right|_{\bar{t}_n}. \quad (75)$$

The dissociation rate estimated in this manner is to be compared with the initial dissociation rate $v_{\text{step } 2}^{\text{diss}}(0) = -dP_{\text{bound}}/dt|_{t=0}$, evaluated at $t=0$, i.e., at the beginning of the propagation, for the calculation of step 2 alone with the phase $\delta=0$. It is found that the values of $-dP_{\text{bound}}/dt|_{\bar{t}_n}$, obtained within the dips exhibited by P_{bound} in the results of the full calculation, are less than the dissociation rate $v_{\text{step } 2}^{\text{diss}}(0)$. In fact, the value of $v_{\text{step } 2}^{\text{diss}}(0)$ is more than twice the average value of $-dP_{\text{bound}}/dt|_{\bar{t}_n}$, as

$$v_{\text{step } 2}^{\text{diss}}(0) = 2.659 \times 10^{-4} \text{ (a.u.)}^{-1},$$

$$\left\langle -\left. \frac{dP_{\text{bound}}}{dt} \right|_{\bar{t}_n} \right\rangle = 1.005 \times 10^{-4} \text{ (a.u.)}^{-1}.$$

These estimates indicate at least that no increase in the dissociation rate accompanies the wave-packet localization due to the continuous ionization. It is in this sense that, with

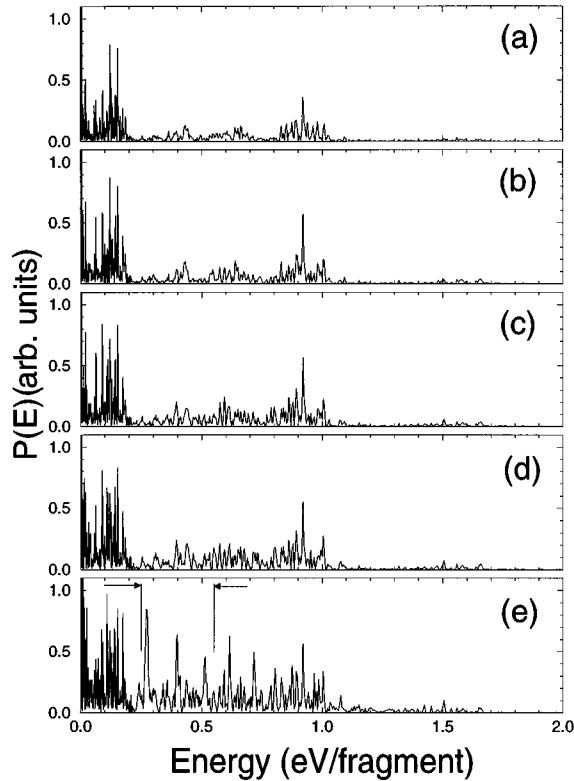


FIG. 8. Kinetic energy spectra of the dissociated fragments of H_2^+ in the center-of-mass frame for (a) $t = 17T_L$, (b) $t = 18T_L$, (c) $t = 19T_L$, (d) $t = 20T_L$, (e) $t = t_f = 1200$ fs. In panel (e), the arrows indicate the range of the experimentally observed kinetic energies of the H^+ fragments.

respect to the dissociation of the ion, there seems to be a stabilization above and beyond that observed in the study of step 2 alone.

A final, noteworthy observation is that the wave-packet localization effect appears to be correlated with the nonadiabatic dynamics illustrated in Fig. 6. The wave packet supported by the upper adiabatic channel ϵ_+ at peak intensity [panels (b) and (d) of Fig. 6] lies within the dissociative continua of the ion as viewed in the diabatic, field-free representation. As the field amplitude decreases toward zero, this wave packet is transferred back to the lower adiabatic potential ϵ_- before it has time to move toward larger internuclear distances.

In summary, a localized, trapped component of the wave packet is found in the dissociative continua of H_2^+ at all times and reflects the continuous population transfer from the neutral ground state to the ionic channels. No enhancement in the dissociation rate of the ion, which would effectively result from this continuous population transfer, is observed.

The existence of a trapped continuum component in the wave packets is further corroborated by the spectra in Fig. 8, which show how the distribution of the kinetic energy of the dissociation products evolve in time. In panel (a), a stable structure of this spectrum starts to emerge after 17 optical cycles, and this structure, consisting notably of a set of high-energy lines in the region 0.6–1.2 eV (per fragment) is preserved thereafter during the action of the laser field, panels (b)–(d). Especially noticeable in panels (c) and (d) is a

single, prominent, narrow peak centered at approximately 0.9 eV (per fragment), which may be associated with the fast dissociative component of the wave packets newly promoted onto the ionic channels each time the field attains its maximum amplitude. In addition, a set of well-defined peaks is found at low energies in all these spectra and may be due to leakage of a portion of the wave packet trapped in the well of the lower adiabatic potential. Once the pulse is over, panel (e), a large number of new lines emerge. These lines can only come from a relaxation of those parts of the wave packets that belong to the dissociation continuum and that were trapped, i.e., localized in the internal region, by the fluctuating electric field. This interpretation is consistent with the fact that, in the two-state study of step 2 alone, the kinetic energy spectrum of the fragments retains its form after the pulse is over while the bound-state and localized populations defined above are indistinguishable at all times.

Previous experiments on the dissociative ionization of H_2 under a 10.6- μm laser pulse gave a typical spectrum that, within the resolution then attainable, was interpreted as a wide distribution of the proton kinetic energy about a single nominal value. The range of this peak value, as observed over 100 laser shots at $I = 5 \times 10^{13}$ W/cm^2 [12], is indicated by the pair of arrows in panel (e) of Fig. 8. The typical experimental fragment kinetic energy spectrum, thus considered monoenergetic, was rationalized in terms of the complete Coulomb explosion of H_2 . In comparison, the calculated spectrum covers a larger range of fragment kinetic energies and is characterized by a complex line structure. New experimental developments have been brought to our attention [41], in which refined experimental methodologies allowed higher-resolution proton kinetic energy spectra to be obtained. Preliminary results [41] of this new experimental work reveal structured spectra that cover the entire range of kinetic energies illustrated in Fig. 8. Meanwhile, the analysis of the structures observed in the experimental and theoretical spectra is being made and an interpretation of these structures in terms of a Floquet picture is being examined. This work is planned for future publication. The present results, obtained from calculations that include only step 1 and step 2 of Fig. 1, show that the dissociation of H_2^+ can produce H^+ fragments with kinetic energies in the experimental range without the further ionization of H_2^+ . However, since step 3 has not been included in the calculation, its relevance in the interpretation of the experimental spectra, as suggested by the complete Coulomb explosion picture of Fig. 1, has yet to be established.

VI. SUMMARY AND CONCLUSIONS

Electron tunneling processes corresponding to the successive ionizations of H_2 induced by an intense low-frequency field have been expressed in terms of field-free BO PES's. To achieve this goal, a projection of the new time-dependent adiabatic electronic states associated with the distorted Coulomb potential, the electron-nuclei potential, plus the instantaneous radiative interaction potential onto the field-free states is needed. This is done by using the time-dependent electronic basis defined by Eq. (6). Essentially, the construction of this basis amounts to recognizing that electrons ionized during the action of the laser pulse are not free but

continue to feel the driving force of the field. By treating the ionized electrons in this manner while the bound ones are still described by field-free BO electronic states, an asymmetry is introduced in the theory. This asymmetry is precisely what is needed to allow for a discussion of the tunnel ionization processes in terms of field-free electronic states. Due to its interaction with the radiation field, an ionized electron described in this basis can have negative total energy. As a consequence, when dressed by the continuous ejected electron energy, the BO PES's of the ionic channels can be brought into resonance with the ground state of the parent species. In this way, the tunnel ionization process, a shape-resonance problem, has been transformed into a Feshbach resonance problem.

Even when the parent molecule and the bound ionic species are each described by a single electronic state, this problem originally involves the interaction between an electronic manifold (PES) of the parent molecule and at least one continuous series of PES's associated with the ionic species, which is accompanied by an ionized electron of energy E . This requires a technique for wave-packet propagation on a continuum of coupled electronic manifolds. A reduction of the wave-packet propagation scheme to an effective five-channel problem has been obtained for the description of the first dissociative ionization process in H₂ by using Fano's formalism to analytically diagonalize the infinite, continuous interaction potential matrix and by using the properties of Fano's solutions. More precisely, the property of Fano's solutions that permits such a reduction is the well-known localization of bound-free population exchanges to "on-the-energy-shell" transitions in the neighborhood of Feshbach resonances. This localization demands that the bound-free couplings do not vary too rapidly with respect to the continuous energy variable, and that they are not so strong that the Feshbach resonances do not overlap appreciably. These conditions are well met in the case of the first ionization of H₂, which occurs mainly in the neighborhood of the neutral equilibrium geometry, where the ground-state population initially resides. In contrast, the second ionization, i.e., the ionization of H₂⁺, is expected to occur at larger internuclear distances, as found in recent investigations of an ionization-enhancement effect [7,9]. In this case, both conditions will not be met, and a reduction of the wave-packet propagation scheme to an effective problem involving a finite number of channels will not be obtained. It is in this respect that the inclusion of the second ionization of H₂, i.e., of step 3 in Fig. 1, constitutes the main challenge for future work, while refinements such as the generation and use of more accurate bound-free matrix elements or the inclusion of rotations in the wave-packet dynamics will, in comparison, be much more straightforward. This is not to say that these refinements are not important and can be neglected. Another point that would require particular attention when the present work is generalized to much higher field intensities and to a higher frequency regime is the participation of excited states of the parent molecule to the dynamics of the dissociative ionization process. These aspects, in particular the adaptation of the present wave-packet formulation to the second ionization of H₂, are being considered in ongoing research.

Presently, only the first dissociative ionization step in the complete sequence of events leading to the Coulomb explo-

sion of H₂ has been studied. The dynamics of the ion under the influence of the continuous ionization process are less adiabatic than those observed in the case of sudden ionization, step 2 alone. In addition, continuous ionization appears to temporarily give a trapped, i.e., a spatially localized wave-packet component belonging to the dissociative continuum, enhancing the stabilization of the ion with respect to dissociation. Although this enhancement is not very large, its presence, together with the more pronounced nonadiabaticity in the wave-packet dynamics, indicates that interference between portions of the wave packets that are promoted on the ionic ground-state at different times during continuous ionization plays an important role, and denotes a strong coupling between the ionization and dissociation events, which are both induced by the laser field.

ACKNOWLEDGMENTS

The authors wish to thank Professor S. L. Chin and Dr. F. Ilkov for stimulating discussions, L. Strach, T. Walsh, and Professor S. L. Chin for communicating new experimental findings prior to their publication (Ref. [42]). Financial support of this research by the Natural Science and Engineering Research Council of Canada (NSERC) and by Québec's Fonds pour la Formation de Chercheurs et l'Aide à la Recherche (FCAR) are gratefully acknowledged. This research was also supported by the joint Québec-France cooperative program "Coopération France-Québec: Recherche et Enseignement Supérieur" through Grant No. 01-03-92.

APPENDIX A

To proceed further from Eqs. (39a)–(39c), analytical expressions for the integrals defined in Eqs. (40a)–(40c) and Eqs. (41a)–(41c) are needed. The present Appendix gives the details of the evaluations of these integrals using contour integrations. For convenience, in the following, $\zeta(E)$ will denote the function

$$\zeta(E) = (|\tilde{v}_E - E\tilde{S}_{-,E}|^2 + |\tilde{w}_E - E\tilde{S}_{+,E}|^2). \quad (\text{A1})$$

Evaluation of I_{aa}

For I_{aa} , substitution of Eq. (35) for $|a_1(E)|^2$ into Eq. (40a) gives

$$I_{aa}(\delta t) = \int dE \frac{\zeta(E) e^{-iE\delta t/\hbar}}{[E - \epsilon_0 - G(E)]^2 + \pi^2 \zeta(E)^2}. \quad (\text{A2})$$

If $\tilde{v}_{E'} - E\tilde{S}_{-,E'}$ and $\tilde{w}_{E'} - E\tilde{S}_{+,E'}$ are slowly varying with respect to E and E' , viewed as complex variables, Eqs. (42) and (43), then the integrand in the above has only a single pole in each half plane of the complex plane. In the lower half plane, this pole is approximately at

$$E = \epsilon_0^{\text{res}} = \epsilon_0 + G(\epsilon_0) - i\Gamma, \quad (\text{A3})$$

where

$$\Gamma = \pi \zeta(\epsilon_0). \quad (\text{A4})$$

$$I_{aa}(\delta t) = e^{-i\epsilon_0^{\text{res}} \delta t / \hbar}. \quad (\text{A5})$$

The integral I_{aa} can then be evaluated using the residue theorem and the contour of Fig. 9(a). The result is

$$I_{ba}(E', \delta t) = I_1(E', \delta t) + \frac{[E' + \epsilon_- - \epsilon_0 - G(E' + \epsilon_-)] [\tilde{v}_{E'+\epsilon_-} - (E' + \epsilon_-) \tilde{S}_{-E'+\epsilon_-}]}{\zeta(E' + \epsilon_-)} |a_1(E' + \epsilon_-)|^2 e^{-i(E'+\epsilon_-)\delta t/\hbar}, \quad (\text{A6})$$

where the second term arises from the $Z(E) \delta(E - E' - \epsilon_-)$ factor in Eq. (29b), after substitution of Eq. (30) for $Z(E)$, while

$$I_1 = \mathcal{P} \int dE \frac{(\tilde{v}_{E'+\epsilon_-} - E \tilde{S}_{-E'+\epsilon_-}) |a_1(E)|^2 e^{-iE\delta t/\hbar}}{E - (E' + \epsilon_-)}. \quad (\text{A7})$$

Within the approximation made above, the integrand in this has a single pole, that of $|a_1(E)|^2$, on the lower half plane, so that using the contour of Fig. 9(b), it is found that

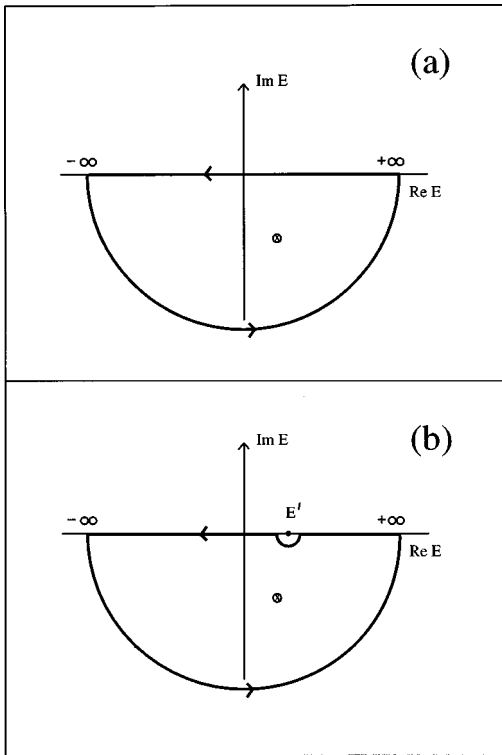


FIG. 9. Integration contours used in evaluation of (a) $I_{aa}(\delta t)$ and (b) integrals involving $P/(E - E')$ in $I_{ba}(E', \delta t)$, $I_{ca}(E', \delta t)$, $I_{\alpha\beta}(E', E'', \delta t)$, $\alpha, \beta = b$ or c . The single pole of $|a_1(E)|^2$ found in the lower complex half plane is indicated in both panels symbolically by \otimes .

Integrals I_{ba} and I_{ca}

Substituting Eqs. (27) and (29b) into the definition of I_{ba} , Eq. (40b) first yields

$$I_1 = \frac{(\tilde{v}_{E'+\epsilon_-} - \epsilon_0^{\text{res}} \tilde{S}_{-E'+\epsilon_-}) e^{-i\epsilon_0^{\text{res}} \delta t / \hbar}}{\epsilon_0^{\text{res}} - (E' + \epsilon_-)} - i\pi |a_1(E' + \epsilon_-)|^2 \times [\tilde{v}_{E'+\epsilon_-} - (E' + \epsilon_-) \tilde{S}_{-E'+\epsilon_-}] e^{-i(E'+\epsilon_-)\delta t/\hbar}. \quad (\text{A8})$$

Substituting this back into Eq. (A6) yields

$$I_{ba} = \frac{(\tilde{v}_{E'+\epsilon_-} - \epsilon_0^{\text{res}} \tilde{S}_{-E'+\epsilon_-}) e^{-i\epsilon_0^{\text{res}} \delta t / \hbar}}{\epsilon_0^{\text{res}} - (E' + \epsilon_-)} + |a_1(E' + \epsilon_-)|^2 \times [\tilde{v}_{E'+\epsilon_-} - (E' + \epsilon_-) \tilde{S}_{-E'+\epsilon_-}] \times e^{-i(E'+\epsilon_-)\delta t/\hbar} \left(\frac{E' + \epsilon_- - \epsilon_0 - G(E' + \epsilon_-)}{\zeta(E' + \epsilon_-)} - i\pi \right). \quad (\text{A9})$$

Substituting Eq. (35) for $|a_1(E)|^2$ into the second term on the right-hand side of the above gives

$$I_{ba} = \frac{(\tilde{v}_{E'+\epsilon_-} - \epsilon_0^{\text{res}} \tilde{S}_{-E'+\epsilon_-}) e^{-i\epsilon_0^{\text{res}} \delta t / \hbar}}{\epsilon_0^{\text{res}} - (E' + \epsilon_-)} + \frac{[\tilde{v}_{E'+\epsilon_-} - (E' + \epsilon_-) \tilde{S}_{-E'+\epsilon_-}] e^{-i(E'+\epsilon_-)\delta t/\hbar}}{(E' + \epsilon_-) - [\epsilon_0 + G(E' + \epsilon_-) - i\pi \zeta(E' + \epsilon_-)]}. \quad (\text{A10})$$

Due to the localized character of the Lorentzian-shaped functions $[\epsilon_0^{\text{res}} - (E' + \epsilon_-)]^{-1}$, $[\epsilon_0 - (E' + \epsilon_-) + G(E' + \epsilon_-) - i\pi \zeta(E' + \epsilon_-)]^{-1}$, which appear in Eq. (A10), and the assumed weak dependence of the bound-free couplings on E , Eqs. (42) and (43), it is possible to rewrite the above in either of the following final forms:

$$I_{ba}(E', \delta t) = (\tilde{v}_{E'+\epsilon_-} - \epsilon_0^{\text{res}} \tilde{S}_{-E'+\epsilon_-}) F(\delta t | \epsilon_0, E' + \epsilon_-), \quad (\text{A11})$$

$$I_{ba}(E', \delta t) = [\tilde{v}_{E'+\epsilon_-} - (E' + \epsilon_-)\tilde{S}_{-E'+\epsilon_-}] \times F(\delta t | \epsilon_0, E' + \epsilon_-), \quad (\text{A12})$$

$$I_{ca}(E', \delta t) = [\tilde{w}_{E'+\epsilon_+} - (E' + \epsilon_+)\tilde{S}_{+E'+\epsilon_+}] \times F(\delta t | \epsilon_0, E' + \epsilon_+). \quad (\text{A14})$$

where

$$F(\delta t | \epsilon_0, E' + \epsilon_{\pm}) \equiv \frac{e^{-i\epsilon_0^{\text{res}} \delta t / \hbar} - e^{-i(E' + \epsilon_{\pm}) \delta t / \hbar}}{\epsilon_0^{\text{res}} - (E' + \epsilon_{\pm})}. \quad (\text{A13})$$

Similarly, the integral I_{ca} is found to reduce simply to

Integrals $I_{\alpha\beta}^{(k)}$, $\alpha, \beta = b, c$, $k = 1, 2$

The evaluations of the integrals $I_{bb}^{(k)}$, $I_{bc}^{(k)}$, and $I_{cc}^{(k)}$ are somewhat more tedious. The details are given here for the evaluations of $I_{bb}^{(k)}$ only.

Substituting Eqs. (27) and (29b) into the definition of $I_{bb}^{(1)}$, Eq. (41a), we have

$$\begin{aligned} I_{bb}^{(1)} = & \mathcal{P} \int dE \frac{(\tilde{v}_{E'+\epsilon_-} - E\tilde{S}_{-,E'+\epsilon_-})(\tilde{v}_{E''+\epsilon_-} - E\tilde{S}_{-,E''+\epsilon_-})^*}{(E - E' - \epsilon_-)(E - E'' - \epsilon_-)} |a_1(E)|^2 e^{-iE\delta t/\hbar} + \mathcal{P} \int dE (\tilde{v}_{E'+\epsilon_-} - E\tilde{S}_{-,E'+\epsilon_-}) \\ & \times (\tilde{v}_{E''+\epsilon_-} - E\tilde{S}_{-,E''+\epsilon_-})^* |a_1(E)|^2 e^{-iE\delta t/\hbar} \left\{ \frac{Z(E)}{E - E'' - \epsilon_-} \delta(E - E' - \epsilon_-) + \frac{Z(E)}{E - E' - \epsilon_-} \delta(E - E'' - \epsilon_-) \right\} \\ & + \int dE (\tilde{v}_{E'+\epsilon_-} - E\tilde{S}_{-,E'+\epsilon_-})(\tilde{v}_{E''+\epsilon_-} - E\tilde{S}_{-,E''+\epsilon_-})^* Z^2(E) \delta(E - E' - \epsilon_-) \delta(E - E'' - \epsilon_-) |a_1(E)|^2 e^{-iE\delta t/\hbar}. \end{aligned} \quad (\text{A15})$$

In the first integral on the right-hand side, we use

$$\begin{aligned} \frac{\mathcal{P}}{(E' + \epsilon_- - E)(E'' + \epsilon_- - E)} &= \frac{\mathcal{P}}{E' - E''} \left\{ \frac{\mathcal{P}}{(E'' + \epsilon_- - E)} - \frac{\mathcal{P}}{(E' + \epsilon_- - E)} \right\} \\ &+ \pi^2 \delta(E' - E'') \delta(E - \tfrac{1}{2}[E' + E'' + 2\epsilon_-]) \end{aligned} \quad (\text{A16})$$

to obtain

$$\begin{aligned} I_{bb}^{(1)} = & \frac{\mathcal{P}}{E' - E''} \left[\mathcal{P} \int dE \frac{(\tilde{v}_{E'+\epsilon_-} - E\tilde{S}_{-,E'+\epsilon_-})(\tilde{v}_{E''+\epsilon_-} - E\tilde{S}_{-,E''+\epsilon_-})^* \zeta(E)}{(E'' + \epsilon_- - E) |E - \epsilon_0 - G(E) - i\pi\zeta(E)|^2} e^{-iE\delta t/\hbar} \right. \\ & \left. - \mathcal{P} \int dE \frac{(\tilde{v}_{E'+\epsilon_-} - E\tilde{S}_{-,E'+\epsilon_-})(\tilde{v}_{E'+\epsilon_-} - E\tilde{S}_{-,E''+\epsilon_-})^* \zeta(E)}{(E' + \epsilon_- - E) |E - \epsilon_0 - G(E) - i\pi\zeta(E)|^2} e^{-iE\delta t/\hbar} \right] \\ & + \pi^2 \delta(E' - E'') |\tilde{v}_{E'+\epsilon_-} - (E' + \epsilon_-)\tilde{S}_{-,E'+\epsilon_-}|^2 |a_1(E' + \epsilon_-)|^2 e^{-i(E'+\epsilon_-)\delta t/\hbar} + \mathcal{P} [\tilde{v}_{E'+\epsilon_-} - (E' + \epsilon_-)\tilde{S}_{-,E'+\epsilon_-}] \\ & \times [\tilde{v}_{E''+\epsilon_-} - (E'' + \epsilon_-)\tilde{S}_{-,E''+\epsilon_-}]^* |a_1(E' + \epsilon_-)|^2 \left\{ \frac{Z(E' + \epsilon_-)}{E' - E''} \right\} e^{-i(E'+\epsilon_-)\delta t/\hbar} - \mathcal{P} [\tilde{v}_{E'+\epsilon_-} - (E'' + \epsilon_-)\tilde{S}_{-,E'+\epsilon_-}] \\ & \times [\tilde{v}_{E''+\epsilon_-} - (E'' + \epsilon_-)\tilde{S}_{-,E''+\epsilon_-}]^* |a_1(E'' + \epsilon_-)|^2 \left\{ \frac{Z(E'' + \epsilon_-)}{E' - E''} \right\} e^{-i(E''+\epsilon_-)\delta t/\hbar} + |\tilde{v}_{E'+\epsilon_-} - (E' + \epsilon_-)\tilde{S}_{-,E'+\epsilon_-}|^2 \\ & \times Z^2(E' + \epsilon_-) |a_1(E' + \epsilon_-)|^2 e^{-i(E'+\epsilon_-)\delta t/\hbar} \delta(E' - E''). \end{aligned} \quad (\text{A17})$$

In the first two terms of this long expression, i.e., in the two integrals that remain to be evaluated, the expression for $|a_1 E|^2$, Eq. (35), has been used to exhibit the analytical properties of the integrands. These integrals can be evaluated by contour integration using the contour of Fig. 9(b), and yield

$$\begin{aligned}
& \mathcal{P} \int dE \frac{(\tilde{v}_{E'+\epsilon_-} - E\tilde{S}_{-,E'+\epsilon_-})(\tilde{v}_{E''+\epsilon_0} - E\tilde{S}_{-,E''+\epsilon_-})^* \zeta(E)}{(\bar{E} + \epsilon_- - E)|E - \epsilon_0 - G(E) - i\pi\zeta(E)|^2} e^{-iE\delta t/\hbar} \\
&= \frac{(\tilde{v}_{E'+\epsilon_-} - \epsilon_0^{\text{res}}\tilde{S}_{-,E'+\epsilon_-})(\tilde{v}_{E''+\epsilon_-} - \epsilon_0^{\text{res}}\tilde{S}_{-,E''+\epsilon_-})^*}{(\bar{E} + \epsilon_- - \epsilon_0^{\text{res}})} e^{-i\epsilon_0^{\text{res}}\delta t/\hbar} - i\pi[\tilde{v}_{E'+\epsilon_-} - (\bar{E} + \epsilon_-)\tilde{S}_{-,E'+\epsilon_-}] \\
&\quad \times [\tilde{v}_{E''+\epsilon_-} - (\bar{E} + \epsilon_-)\tilde{S}_{-,E''+\epsilon_-}]^* |a_1(\bar{E} + \epsilon_-)|^2 e^{-i(\bar{E} + \epsilon_-)\delta t/\hbar}, \tag{A18}
\end{aligned}$$

where $\bar{E} = E'$ or E'' . Substituting these results into Eq. (A17) and using Eqs. (35) and (30) for $|a_1(E)|^2$ and $Z(E)$, respectively, we finally obtain, after some lengthy but straightforward algebraic rearrangements,

$$\begin{aligned}
I_{bb}^{(1)}(E', E'') &= \frac{\mathcal{P}}{E' - E''} (\tilde{v}_{E'+\epsilon_-} - \epsilon_0^{\text{res}}\tilde{S}_{-,E'+\epsilon_-})(\tilde{v}_{E''+\epsilon_-} - \epsilon_0^{\text{res}}\tilde{S}_{-,E''+\epsilon_-})^* \{F(\delta t|\epsilon_0, E' + \epsilon_-) - F(\delta t|\epsilon_0, E'' + \epsilon_-)\} \\
&\quad + \delta(E' - E'') \frac{|\tilde{v}_{E'+\epsilon_-} - (E' + \epsilon_-)\tilde{S}_{-,E'+\epsilon_-}|^2 e^{-i(E'+\epsilon_-)\delta t/\hbar}}{\zeta(E' + \epsilon_-)}. \tag{A19}
\end{aligned}$$

Again, due to the localized character of the function $F(\delta t|\epsilon_0, E' + \epsilon_-)$, and the weak E dependence of the bound-free couplings, Eqs. (42) and (43), we can rewrite this in the following simpler, final form:

$$\begin{aligned}
I_{bb}^{(1)}(E', E'') &= \mathcal{P} \frac{|\tilde{v}_{E'+\epsilon_-} - \epsilon_0^{\text{res}}\tilde{S}_{-,E'+\epsilon_-}|^2}{E' - E''} \{F(\delta t|\epsilon_0, E' + \epsilon_-) - F(\delta t|\epsilon_0, E'' + \epsilon_-)\} + \delta(E' - E'') \\
&\quad \times \frac{|\tilde{v}_{E'+\epsilon_-} - (E' + \epsilon_-)\tilde{S}_{-,E'+\epsilon_-}|^2 e^{-i(E'+\epsilon_-)\delta t/\hbar}}{\zeta(E' + \epsilon_-)}. \tag{A20}
\end{aligned}$$

Adding to this result the integral $I_{bb}^{(2)}$, which, according to Eqs. (27) and (32b) is simply

$$I_{bb}^{(2)}(E', E'') = \delta(E' - E'') \frac{|\tilde{w}_{E'+\epsilon_-} - (E' + \epsilon_-)\tilde{S}_{+,E'+\epsilon_-}|^2 e^{-i(E'+\epsilon_-)\delta t/\hbar}}{\zeta(E' + \epsilon_-)} \tag{A21}$$

we have

$$\sum_k I_{bb}^{(k)}(E', E'') = \mathcal{P} \frac{|\tilde{v}_{E'+\epsilon_-} - \epsilon_0^{\text{res}}\tilde{S}_{-,E'+\epsilon_-}|^2}{E' - E''} \{F(\delta t|\epsilon_0, E' + \epsilon_-) - F(\delta t|\epsilon_0, E'' + \epsilon_-)\} + \delta(E' - E'') e^{-i(E'+\epsilon_-)\delta t/\hbar}. \tag{A22}$$

Similarly, it is found that

$$\sum_k I_{cc}^{(k)}(E', E'') = \mathcal{P} \frac{|\tilde{w}_{E'+\epsilon_+} - \epsilon_0^{\text{res}}\tilde{S}_{+,E'+\epsilon_+}|^2}{E' - E''} \{F(\delta t|\epsilon_0, E' + \epsilon_+) - F(\delta t|\epsilon_0, E'' + \epsilon_+)\} + \delta(E' - E'') e^{-i(E'+\epsilon_+)\delta t/\hbar} \tag{A23}$$

and

$$\sum_k I_{bc}^{(k)}(E', E'') = \mathcal{P} \frac{(\tilde{v}_{E'+\epsilon_-} - \epsilon_0^{\text{res}}\tilde{S}_{-,E'+\epsilon_-})(\tilde{w}_{E''+\epsilon_+} - \epsilon_0^{\text{res}}\tilde{S}_{+,E''+\epsilon_+})^*}{E' - E'' + \epsilon_- - \epsilon_+} \{F(\delta t|\epsilon_0, E' + \epsilon_-) - F(\delta t|\epsilon_0, E'' + \epsilon_+)\}. \tag{A24}$$

APPENDIX B

Appendix A gives the final expressions for the various integrals appearing in Eqs. (39a)–(39c). These results were obtained within the approximation that the bound-free matrix elements are slowly varying with respect to the energy of the ionized electron, Eqs. (42) and (43). The present Appendix deals with the use of these expressions to obtain the results reported in Eqs. (46a)–(46c). While Eq. (46a) follows straightforwardly from Eq. (39a) using the results of Eqs. (A5), (A12), and (A14), the substitutions of Eqs. (A22), (A23), (A24), and (A12) into Eqs. (39b) and (39c) do not yield Eqs. (46b) and (46c) directly. For example, consider the wave packet $\chi_{1E'}$ belonging to the continuum associated with the ground state of the H_2^+ ion. We first obtain, within the same approximation as in Eq. (42):

$$\begin{aligned}
\chi_{1E'}(R, t_0 + \delta t) = & \eta_{1E'}(R, t_0 + \delta t) + e^{-(i/\hbar)E'\delta t} e^{-(i/\hbar)\hat{T}_N\delta t/2} \{ \cos\theta e^{-(i/\hbar)\epsilon_-\delta t} [\cos\theta e^{-(i/\hbar)\hat{T}_N\delta t/2} \chi_{1E'}(R, t_0) \\
& - \sin\theta e^{-(i/\hbar)\hat{T}_N\delta t/2} \chi_{2E'}(R, t_0)] \} + e^{-(i/\hbar)E'\delta t} e^{-(i/\hbar)\hat{T}_N\delta t/2} \{ \sin\theta e^{-(i/\hbar)\epsilon_+\delta t} [\sin\theta e^{-(i/\hbar)\hat{T}_N\delta t/2} \chi_{1E'}(R, t_0) \\
& + \cos\theta e^{-(i/\hbar)\hat{T}_N\delta t/2} \chi_{2E'}(R, t_0)] \} + e^{-(i/\hbar)\hat{T}_N\delta t/2} \left\{ \cos|\tilde{v}_{\epsilon_0} - \epsilon_0\tilde{S}_{-, \epsilon_0}|^2 \right. \\
& \times \mathcal{P} \int dE'' \frac{F(\delta t|\epsilon_0, E' + \epsilon_-) - F(\delta t|\epsilon_0, E'' + \epsilon_-)}{E' - E''} [\cos\theta e^{-(i/\hbar)\hat{T}_N\delta t/2} \chi_{1E'}(R, t_0) \\
& - \sin\theta e^{-(i/\hbar)\hat{T}_N\delta t/2} \chi_{2E''}(R, t_0)] + \cos\theta(\tilde{v}_{\epsilon_0} - \epsilon_0\tilde{S}_{-, \epsilon_0})(\tilde{w}_{\epsilon_0} - \epsilon_0\tilde{S}_{+, \epsilon_0})^* \\
& \times \mathcal{P} \int dE'' \frac{F(\delta t|\epsilon_0, E' + \epsilon_-) - F(\delta t|\epsilon_0, E'' + \epsilon_+)}{E' - E'' + \epsilon_- - \epsilon_+} [\sin\theta e^{-(i/\hbar)\hat{T}_N\delta t/2} \chi_{1E''}(R, t_0) \\
& + \cos\theta e^{-(i/\hbar)\hat{T}_N\delta t/2} \chi_{2E''}(R, t_0)] + \sin\theta(\tilde{v}_{\epsilon_0} - \epsilon_0\tilde{S}_{-, \epsilon_0})^*(\tilde{w}_{\epsilon_0} - \epsilon_0\tilde{S}_{+, \epsilon_0}) \\
& \times \mathcal{P} \int dE'' \frac{F(\delta t|\epsilon_0, E' + \epsilon_-) - F(\delta t|\epsilon_0, E'' + \epsilon_+)}{E' - E'' + \epsilon_- - \epsilon_+} [\cos\theta e^{-(i/\hbar)\hat{T}_N\delta t/2} \chi_{1E''}(R, t_0) \\
& - \sin\theta e^{-(i/\hbar)\hat{T}_N\delta t/2} \chi_{2E''}(R, t_0)] + \sin\theta|\tilde{w}_{\epsilon_0} - \epsilon_0\tilde{S}_{+, \epsilon_0}|^2 \\
& \times \mathcal{P} \int dE'' \frac{F(\delta t|\epsilon_0, E' + \epsilon_+) - F(\delta t|\epsilon_0, E'' + \epsilon_+)}{E' - E''} [\sin\theta e^{-(i/\hbar)\hat{T}_N\delta t/2} \chi_{1E''}(R, t_0) \\
& \left. + \cos\theta e^{-(i/\hbar)\hat{T}_N\delta t/2} \chi_{2E''}(R, t_0) \right\}, \tag{B1}
\end{aligned}$$

where

$$\begin{aligned}
\eta_{1E'}(R, t_0 + \delta t) = & e^{-(i/\hbar)\hat{T}_N\delta t/2} \{ \cos\theta [v_{E'} - (E' + \epsilon_-) S_{-E'}] F(\delta t|\epsilon_0, E' + \epsilon_-) + \sin\theta [w_{E'} - (E' + \epsilon_+) S_{+E'}] \\
& \times F(\delta t|\epsilon_0, E' + \epsilon_+) \} e^{-(i/\hbar)\hat{T}_N\delta t/2} \chi_0(R, t_0). \tag{B2}
\end{aligned}$$

The first part of the above lengthy expression, Eq. (B1), represents what would be obtained if the integrals $I_{bb}^{(1)}$, $I_{cc}^{(1)}$, and $I_{bc}^{(1)}$ did not contain the nonlocal terms involving the function F in Eqs. (A22) and (A23). It turns out that these nonlocal terms have a vanishing net effect on the propagation scheme. To see this, consider first what happens at the end of the first two time slices. With $t_0=0$, and the physical condition that only the neutral species ground state is populated at this initial moment, i.e., $\chi_0(R, t_0) \neq 0$, while $\chi_{1E}(t=0) = 0 = \chi_{2E}(t=0)$, the above Eq. (B1) gives

$$\chi_{1E'}(R, \delta t) = \eta_{1E'}(R, \delta t) \tag{B3}$$

simply, so that $\chi_{1E'}$ (and $\chi_{2E'}$) are simple linear combinations of the functions $F(\delta t|\epsilon_0, E' + \epsilon_{\pm})$. Now, these continuum wave functions are part of the initial conditions for the propagation over the second time slice, i.e., from $t_0 = \delta t$ to $t = 2\delta t$. Substituting these expressions into Eq. (B1) gives, in conjunction with the nonlocal terms of $I_{bb}^{(1)}$ and $I_{cc}^{(1)}$, integrals of the form

$$\mathcal{P} \int dE'' \frac{F(\delta t|\epsilon_0, E' + \epsilon_j) - F(\delta t|\epsilon_0, E'' + \epsilon_j)}{E' - E''}$$

$$\times F(\delta t|\epsilon_0, E'' + \epsilon_l), \tag{B4}$$

where $j, l = \pm$ and, in conjunction with the nonlocal terms of $I_{bc}^{(1)}$, integrals of the form

$$\begin{aligned}
& \mathcal{P} \int dE'' \frac{F(\delta t|\epsilon_0, E' + \epsilon_-) - F(\delta t|\epsilon_0, E'' + \epsilon_+)}{E' - E'' + \epsilon_- - \epsilon_+} \\
& \times F(\delta t|\epsilon_0, E'' + \epsilon_l). \tag{B5}
\end{aligned}$$

Due to the localized character of the functions $F(\delta t|\epsilon_0, E' + \epsilon_{\pm})$, viewed as a function of E' , Eq. (B4) is nonzero only when $\epsilon_l = \epsilon_j$, assuming that Γ , Eq. (A4), is small, i.e., that the bound-free couplings are small with respect to the energy separation $|\epsilon_- - \epsilon_+|$. Note that while this would warrant the satisfaction of the conditions of Eqs. (42) and (43), it is not required, or implied by these conditions. Also, in writing Eqs. (B4) and (B5), a commutator between $\exp(-i\hat{T}_N\delta t/2\hbar)$ and $F(\delta t|\epsilon_0, E' + \epsilon_l)$ has been neglected. By referring to the expression of $F(\delta t|\epsilon_0, E' + \epsilon_l)$ given in Eq. (53), this commutator is found to be of order δt^3 , i.e., the same order of magnitude as error terms associated with the split-operator formula itself, and can be consistently neglected. Using the

explicit expressions of $F(\delta t|\epsilon_0, E' + \epsilon_{\pm})$, Eq. (A13), and the following straightforward relations

$$\mathcal{P} \int dE'' \frac{e^{-i(E'' + \epsilon_j)\delta t/\hbar}}{E' - E''} = i\pi e^{-i(E' + \epsilon_j)\delta t/\hbar}, \quad (\text{B6})$$

$$\int dE'' \frac{e^{-i(E'' + \epsilon_j)\delta t/\hbar}}{\epsilon_0^{\text{res}} - (E'' + \epsilon_j)} = 2i\pi e^{-i\epsilon_0^{\text{res}}\delta t/\hbar}, \quad (\text{B7})$$

$$\int dE'' \frac{1}{\epsilon_0^{\text{res}} - (E'' + \epsilon_j)} = i\pi, \quad (\text{B8})$$

it is found that

$$\begin{aligned} & \mathcal{P} \int dE'' \frac{F(\delta t|\epsilon_0, E' + \epsilon_j)F(\delta t|\epsilon_0, E'' + \epsilon_j)}{E' - E''} \\ &= \frac{F(\delta t|\epsilon_0, E' + \epsilon_j)}{\epsilon_0^{\text{res}} - (E' + \epsilon_j)} \int dE'' \left[\frac{\mathcal{P}}{E' - E''} - \frac{1}{\epsilon_0^{\text{res}} - (E'' + \epsilon_j)} \right] \\ & \quad \times (e^{-i\epsilon_0^{\text{res}}\delta t/\hbar} - e^{-i(E'' + \epsilon_j)\delta t/\hbar}) = i\pi [F(\delta t|\epsilon_0, E' + \epsilon_j)]^2 \end{aligned} \quad (\text{B9})$$

and

$$\begin{aligned} & \mathcal{P} \int dE'' \frac{[F(\delta t|\epsilon_0, E'' + \epsilon_j)]^2}{E' - E''} \\ &= \frac{1}{[\epsilon_0^{\text{res}} - (E' + \epsilon_j)]^2} \int dE'' \left[\frac{\mathcal{P}}{E' - E''} - \frac{1}{\epsilon_0^{\text{res}} - (E'' + \epsilon_j)} \right] \\ & \quad \times (e^{-2i\epsilon_0^{\text{res}}\delta t/\hbar} + e^{-2i(E'' + \epsilon_j)\delta t/\hbar} - e^{-i(\epsilon_0^{\text{res}} + E'' + \epsilon_j)\delta t/\hbar}) \\ & \quad - \frac{1}{\epsilon_0^{\text{res}} - (E' + \epsilon_j)} \int dE'' \frac{(e^{-i\epsilon_0^{\text{res}}\delta t/\hbar} - e^{-i(E'' + \epsilon_j)\delta t/\hbar})^2}{[\epsilon_0^{\text{res}} - (E'' + \epsilon_j)]^2} \\ &= i\pi [F(\delta t|\epsilon_0, E' + \epsilon_j)]^2. \end{aligned} \quad (\text{B10})$$

Thus, the integral defined in Eq. (B4) vanishes exactly. As to Eq. (B5), consider $\epsilon_l = \epsilon_-$ for example. Then the second

term in Eq. (B5) is zero due to the vanishing overlap of the two functions F centered at ϵ_+ and ϵ_- . On the other hand, the first term is

$$\begin{aligned} & F(\delta t|\epsilon_0, E' + \epsilon_-) \mathcal{P} \int dE'' \frac{F(\delta t|\epsilon_0, E'' + \epsilon_-)}{E' - E'' + \epsilon_- - \epsilon_+} \\ &= i\pi F(\delta t|\epsilon_0, E' + \epsilon_-) F(\delta t|\epsilon_0, E'' + 2\epsilon_- - \epsilon_+) = 0. \end{aligned} \quad (\text{B11})$$

To obtain this result, it suffices to replace E' in all the terms $1/(E' - E'')$ appearing in Eq. (B9) by $E' + \delta\epsilon$, where $\delta\epsilon = \epsilon_- - \epsilon_+$. Since the two F functions on the right-hand side of Eq. (B11) are centered at very distant energy, their product is virtually zero. Similarly, with $\epsilon_l = \epsilon_+$, the second term of Eq. (B5) is

$$\begin{aligned} & \mathcal{P} \int dE'' \frac{[F(\delta t|\epsilon_0, E'' + \epsilon_+)]^2}{E' - E'' + \delta\epsilon} \\ &= i\pi [F(\delta t|\epsilon_0, E' + \epsilon_+ + \delta\epsilon)]^2 \\ &= i\pi [F(\delta t|\epsilon_0, E' + \epsilon_-)]^2, \end{aligned} \quad (\text{B12})$$

while the first term gives

$$\begin{aligned} & F(\delta t|\epsilon_0, E' + \epsilon_-) \mathcal{P} \int dE'' \frac{F(\delta t|\epsilon_0, E'' + \epsilon_+)}{E' - E'' + \delta\epsilon} \\ &= i\pi F(\delta t|\epsilon_0, E' + \epsilon_-) F(\delta t|\epsilon_0, E' + \epsilon_+ + \delta\epsilon) \\ &= i\pi [F(\delta t|\epsilon_0, E' + \epsilon_-)]^2 \end{aligned} \quad (\text{B13})$$

and the two terms cancel each other exactly.

Summarizing, with respect to wave packets propagated up to the end of the second time slice, the nonlocal terms in $I_{bb}^{(1)}$, $I_{cc}^{(1)}$, and $I_{bc}^{(1)}$ give a net effect that is vanishingly small. The demonstration of this result rests on the fact that $\chi_{1E'}$ and $\chi_{2E'}$ at the beginning of the second slice are linear combinations of the functions F , which give a localization of these wave packets in two narrow intervals of the energy scale. It can easily be seen by recursion that this qualitative trait of $\chi_{1E'}$ and $\chi_{2E'}$ will be preserved at all times, so that the analysis made above can be generalized to an arbitrary time slice, yielding the general conclusion that the nonlocal terms of $I_{bb}^{(1)}$, $I_{cc}^{(1)}$, and $I_{bc}^{(1)}$ remain ineffective at all times. Thus Eq. (B1) reduces to

$$\begin{aligned} \chi_{1E'}(R, t_0 + \delta t) &= \eta_{1E'}(R, t_0 + \delta t) + e^{-(i/\hbar)E'\delta t} e^{-(i/\hbar)\hat{T}_N\delta t/2} \\ & \quad \times \{ \cos\theta e^{-(i/\hbar)\epsilon_-\delta t} \\ & \quad \times [\cos\theta e^{-(i/\hbar)\hat{T}_N\delta t/2} \chi_{1E'}(R, t_0) - \sin\theta e^{-(i/\hbar)\hat{T}_N\delta t/2} \chi_{2E'}(R, t_0)] \\ & \quad + e^{-(i/\hbar)E'\delta t} e^{-(i/\hbar)\hat{T}_N\delta t/2} \{ \sin\theta e^{-(i/\hbar)\epsilon_+\delta t} [\sin\theta e^{-(i/\hbar)\hat{T}_N\delta t/2} \chi_{1E'}(R, t_0) \\ & \quad + \cos\theta e^{-(i/\hbar)\hat{T}_N\delta t/2} \chi_{2E'}(R, t_0)] \}, \end{aligned} \quad (\text{B14})$$

which is the result reported in Eq. (46b). A similar treatment of the detailed expression of $\chi_{2E'}$ gives the reduced form reported in Eq. (46c).

- [1] K. Codling and L. J. Frasinski, *J. Phys. B* **26**, 783 (1993).
- [2] C. Cornaggia, J. Lavancier, D. Normand, J. Morellec, and H. Liu, *Phys. Rev. A* **42**, 5464 (1990).
- [3] D. T. Strickland, Y. Beaudoin, P. Dietrich, and P. Corkum, *Phys. Rev. Lett.* **68**, 2755 (1992).
- [4] M. Schmidt, D. Normand, and C. Cornaggia, *Phys. Rev. A* **50**, 5037 (1994).
- [5] D. Normand and M. Schmidt, *Phys. Rev. A* **53**, R1958 (1996).
- [6] M. Schmidt, P. D'Oliveira, P. Meynadier, D. Normand, and C. Cornaggia, *Int. J. Nonlinear Opt. Phys.* **4**, 817 (1995).
- [7] T. Zuo and A. D. Bandrauk, *Phys. Rev. A* **52**, R2511 (1995).
- [8] S. Chelkowski, T. Zuo, O. Atabek, and A. D. Bandrauk, *Phys. Rev. A* **52**, 2977 (1995).
- [9] T. Seideman, M. Y. Ivanov, and P. B. Corkum, *Phys. Rev. Lett.* **75**, 2819 (1995).
- [10] T. Seideman, M. Y. Ivanov, and P. B. Corkum, *Chem. Phys. Lett.* **252**, 181 (1996).
- [11] E. Constant, H. Stapelfeldt, and P. B. Corkum, *Phys. Rev. Lett.* **76**, 4140 (1996).
- [12] F. Ilkov, T. D. G. Walsh, S. Turgeon, and S. L. Chin, *Phys. Rev. A* **51**, R2695 (1995).
- [13] F. Ilkov, S. Turgeon, T. D. G. Walsh, and S. L. Chin, *Chem. Phys. Lett.* **247**, 1 (1995).
- [14] M. V. Ammosov, N. B. Delone, and V. P. Krainov, *Zh. Eksp. Teor. Fiz.* **91**, 2208 (1986) [*Sov. Phys. JETP* **64**, 1191 (1986)].
- [15] M. E. Goggin and P. W. Milonni, *Phys. Rev. A* **37**, 796 (1988).
- [16] M. Thachuk and D. M. Wardlaw, *J. Chem. Phys.* **102**, 7462 (1995).
- [17] F. Châteauneuf, T. T. Nguyen-Dang, O. Atabek, A. Keller, F. A. Ilkov, and S. L. Chin (unpublished).
- [18] H. R. Reiss, *Phys. Rev. A* **22**, 1786 (1980).
- [19] F. H. M. Faisal, *J. Phys. B* **6**, L89 (1973).
- [20] L. V. Keldysh, *Zh. Eksp. Teor. Fiz.* **47**, 1945 (1964) [*Sov. Phys. JETP* **20**, 1307 (1965)].
- [21] H. R. Reiss and V. P. Krainov, *Phys. Rev. A* **50**, R910 (1994).
- [22] M. D. Feit, J. A. Fleck, and A. Steiger, *J. Comput. Phys.* **47**, 410 (1982).
- [23] A. Askar and A. S. Cakmak, *J. Phys. (France)* **68**, 2794 (1978).
- [24] R. Kosloff, *J. Phys. Chem.* **92**, 2087 (1988).
- [25] J. Alvarellos and H. Metiu, *J. Chem. Phys.* **88**, 4957 (1988).
- [26] U. Fano, *Phys. Rev.* **124**, 1866 (1961).
- [27] S. Manoli and T. T. Nguyen-Dang, *Phys. Rev. A* **48**, 4307 (1993).
- [28] The relevant comparison is that of the field frequency ω to the Bohr frequencies of electronic transition.
- [29] As detailed in Sec. V, the wave-packet propagation scheme uses time slices of order 0.05 fs. For a 10.6- μm laser, the electric field amplitude varies by less than 0.1% on this time scale. Thus, over each slice, this electric field can be considered constant, and the electronic basis states \mathcal{A}_E do not vary.
- [30] Just as the eigenstates of the field-free two-electron molecular Hamiltonian are independent, so are the elements of the basis \mathcal{B} . They are not mutually orthogonal however.
- [31] F. L. Pilar, *Elementary Quantum Chemistry* (McGraw-Hill, New York, 1990).
- [32] G. Jolicard and O. Atabek, *Phys. Rev. A* **46**, 5845 (1992).
- [33] H. Abou-Rachid, T. Nguyen-Dang, R. Chaudhury, and X. He, *J. Chem. Phys.* **97**, 5497 (1992).
- [34] T. T. Nguyen-Dang, F. Châteauneuf, O. Atabek, and X. He, *Phys. Rev. A* **51**, 1387 (1995).
- [35] For $R = 1.4$ a.u. and $|\mathcal{E}| = 3.769 \times 10^{-2}$ a.u., the bound-free couplings are estimated to be $(v_{\epsilon_0-\epsilon_-} - \epsilon_0 S_{-, \epsilon_0-\epsilon_-}) = 1 \times 10^{-6}$ a.u. and $(w_{\epsilon_0-\epsilon_+} - \epsilon_0 S_{+, \epsilon_0-\epsilon_+}) = 5.5 \times 10^{-15}$ a.u. This gives $\Gamma = 3.14 \times 10^{-12}$ a.u. and $(\hbar/\Gamma) \approx 10^{12}$ a.u. or 10^{11} fs. By direct numerical differentiation in the neighborhood of $\epsilon_0(R_{\text{eq}})$, the logarithmic derivative $(1/\Gamma)d\Gamma/dE$ has been evaluated to be of the order 10^{-4} .
- [36] R. Heather and H. Metiu, *J. Chem. Phys.* **86**, 5009 (1987).
- [37] A. Keller, *Phys. Rev. A* **52**, 1450 (1995).
- [38] F. V. Bunkin and I. I. Tugov, *Phys. Rev. A* **8**, 601 (1973).
- [39] T. D. G. Walsh, J. E. Decker, and S. L. Chin, *J. Phys. B* **26**, L85 (1993).
- [40] To locate \bar{t}_n , note that the time dependence of the rate $v^{\text{loc}}(t)$ should follow closely that of the rate of ionization $\Gamma(t)$, which is given by Eq. (45). (Recall that this is constant over each time slice, but varies from one time slice to another.) Thus, zeroes of $\Gamma(t)$ are also those of $v^{\text{loc}}(t)$. It turns out that $\Gamma(t)$ exhibits a comblike structure with narrow peaks regularly spaced by half an optical cycle, and occurring at maximum field intensity. The half-width of each peak, i.e., the time interval (within a dip in P_{bound} and P_{loc}) where v^{loc} is not negligible, is 2.7 fs corresponding to 7% of the optical cycle. In contrast, the length of the dips exhibited by P_{bound} and P_{loc} in Fig. 7(b) covers a quarter of the optical cycle. Hence, a \bar{t}_n satisfying Eq. (73a) can always be found within these dips. In fact, at a true zero of $v^{\text{loc}}(t)$, Eq. (71) becomes an equality, and $v^{\text{diss}}(\bar{t}_n)$ can be identified with $-(dP_{\text{loc}}/dt)|_{\bar{t}_n}$. However, any inaccuracy in \bar{t}_n would give an underestimated dissociation rate if v^{diss} is calculated as $-(dP_{\text{loc}}/dt)|_{\bar{t}_n}$. On the other hand, a small deviation of \bar{t}_n from a true zero of v^{loc} will not modify Eq. (74) provided that Eq. (73b) remains true.
- [41] L. Strach, T. D. G. Walsh, and S. L. Chin (private communications).